Microwave absorption of film explained accurately by wave cancellation theory

Ying Liu (yingliusd@163.com)
Shenyang Normal University https://orcid.org/0000-0001-9862-5786
Xiangbin Yin
Shenyang Normal University
M. G. B. Drew
University of Reading - Whiteknights Campus: University of Reading
Yue Liu
Shenyang Normal University

Research Article

Keywords: Transmission-line theory, material characterization, impedance matching, applied physics, solid-state physics

Posted Date: May 12th, 2023

DOI: https://doi.org/10.21203/rs.3.rs-2616469/v2

Version of Record: A version of this preprint was published at Physica B: Condensed Matter on October 1st, 2023. See the published version at https://doi.org/10.1016/j.physb.2023.415108.

Microwave absorption of film explained accurately by wave cancellation theory

Ying Liu[1, *], Xiangbin Yin[1], M. G. B. Drew[2], Yue Liu[1]

[1]College of Chemistry and Chemical Engineering, Shenyang Normal University, Shenyang, P. R. China,110034, yingliusd@163.com (Ying Liu), 1057985820@qq.com (Xiangbin Yin), yueliusd@163.com (Yue Liu), tel: 86-024- 86578790, fax: none

[2]School of Chemistry, The University of Reading, Whiteknights, Reading RG6 6AD, UK, mailto:m.g.b.drew@reading.ac.uk

* Corresponding author

Abstract

It has been proved theoretically that in the field of microwave absorption, film and material are confused, and that the impedance matching theory (IM) which is usually applied to metal-backed film is inadequate. Before the scientific community accepts any new theories, it is necessary to validate them from different perspectives with a variety of experimental data such as those obtained from films of different materials. By analysis of experimental data, it is elaborated here from new perspectives that the problems with IM cannot be solved even if different criteria such as the value of $|Z_{in} - Z_0|$ or the phase difference between Z_{in} and Z_0 are used and therefore it needs to be replaced by wave cancellation theory. The analysis in this work applies to published data and supports the following conclusions. The value of reflection loss *RL* is determined by energy conservation, specific to film since it is related to the amplitude of the resultant of the two beams reflected from the two interfaces in the film, and the angular effect from the phase difference between the two beams is vital for understanding microwave absorption from film.

Keywords

Transmission-line theory; material characterization; impedance matching; applied physics; solid-state physics.

1. Introduction

The microwave absorption properties of material and film are completely different. However, in microwave absorption research the properties of "layered material" or "material with thickness *d*" are often referred to as the properties of material and it is concluded that the property of reflection loss *RL*, which is a property of device, can be used to identify the best absorption material [1-5]. Layered material should be classified as film which is a device composed of a portion of material with two parallel interfaces as shown in Fig A1. These two interfaces introduce back-and-forth reflections within film, and result in beam t together with beam 1_r reflected from the front interface of the film. These features are unique to film and they are responsible for the different absorption properties of film and material. Uniform material behaves as a single phase even if it is composed of nano-particles [6].

When microwaves are incident on a metal-backed film (MB) from the open space as beam i, some will be reflected from the front interface at x_1 as beam 1_r while others will enter the film as beam 1_f which is subsequently reflected back-and-forth between the two interfaces in the film to provide the total forward beam f_M shown in Fig. A1. As a result, a number of beams are reflected back into the open space from the rear interface at $x_2 = x_1 + d$ as 2_r, 3_r, 4_r, etc. (not indicated in Fig. A1) which can be summed as beam t transmitted from the total backward beam b_M.

The main difference between the properties of material and film are that the absorption of the former is a monotonic function of the distance traveled by microwaves while of the latter gives rise to absorption peaks as a function of film thickness d. Attenuation power of material is a constant anywhere in the material and its accumulative effect along the traveling path results in monotonic decay of the intensity as microwaves travel further into the material [6]. The permittivity ε_r and permeability μ_r of open space are real numbers and thus their imaginary parts are zero. Open space does not absorb and therefore microwave absorption of film can be determined from reflection loss $RL(x_1^-)$ which is evaluated from beams 1_r and t at x_1^- (the position immediately before x_1). However, $RL(x_1^-)$/dB is not a monotonic function of d thus it cannot be used to characterize the absorption of material. The multi-peaks $RL(x_1^-)$/dB originate from the fact that the phase of beam t is a function of d and thus the peaks of $RL(x_1^-)$/dB are due to the fact that the phase difference ϕ of beams t and 1_r is periodically out of phase by π as d increases [7, 8]. This provides a good example of the observation that the property of a portion of material is different from that of the material itself while it is believed in current theory that absorption peaks of layed material originate from the material [9] or from its resonances [5, 10-12]. Layered material behaves as film because it can be viewed as a portion of material which has front and back interfaces.

Relevant expressions are fully derived in the Appendix. It is first demonstrated from numerical calculations [7] and then proved theoretically from angular effects [8] that the most efficient absorption takes place when $\phi = (2n + 1)\pi$ resulting in full wave cancellation and the least absorption takes place where $\phi = 2n\pi$, where n is an integer. The absorption from film has nothing to do with the resonance of material. Since the absorption of film is characterized by the cancellation of beams 1_r and t, films providing efficient absorption can be composed of poor absorption material and at absorption peaks, films can absorb more microwaves than can the material alone.

The confusion between film and material has led to the wrong absorption mechanism that it is wrongly believed that the multi-absorption peaks represented by $RL(x_1^-)$/dB originate from material or the resonance of material [9]. Even though the minima of $|RL(x_1^-)|$ can be predicted precisely using a formula derived from transmission-line theory based on wave superposition, the real absorption mechanism concerning beams t and 1_r has never been identified previously in the field of material research as crucial. Instead, it is wrongly believed, based on impedance matching theory (IM), that to increase absorption, it is necessary to allow more microwaves to enter the film and in addition to use suitable material with large attenuation power, a concept established in the accepted theory by the confusion of film and material. As a result, it is commonly speculated that a weaker beam t provides

greater absorption [13]. But these arguments are flawed, being a result of confusion between a film and the material [7, 14, 15].

The cancelation of beams 1_r and t provides the key to differentiate the mechanism of absorption of film from that of material. In fact, for most materials, the imaginary parts of permittivity ε_r'' and permeability μ_r'' are small, and the strongest beam t provides the most efficient absorptions at $\phi = (2n + 1)\pi$ and the weakest provides the least absorption at $\phi = 2n\pi$ [7, 8]. This can be easily understood by considering energy conservation for a film that does not absorb microwaves [8, 14], which involves returning the required energy to the open space by beam t when it is canceled or enhanced by beam 1_r [7, 8]. The more reflections required by the strongest beam t ensure that film can absorb more than material alone. The small values of ε_r'' and μ_r'' prevalent in often-used materials cannot change this result. The amplitude of beam t can be weaker at $\phi = 0$ and then fewer back-and-forth reflections in the film are needed since beam 1_r has already returned some energy to the open space. Only in the case where $\varepsilon_r = \mu_r$ does a film behave like material since then the front interface disappears and the back-and-forth reflections no longer occur. The back-and-forth reflections are the characteristic of film different from material even when $\phi = 0$. Although the optical path produced by back-and-forth reflections is related to absorption, the final response of film is determined by the wave superposition of beams 1_r and t. The absorption in film can be less than that in material when $\phi = 0$

where all the individual beams (2r, 3r, 4r, etc.) represented by t are in phase with beam 1_r.

The back-and-forth reflection cycles within film are related to energy conservation and the wave superposition of beams 1_r and t. Thus, in contrast to material, the number of reflection cycles in film are responsible for its unique absorption property [7, 14]. These new results are derived from physics and can be proved by numerical calculations on the amplitude of beam t [8, 14, 15], which contrasts with the commonly accepted previous proposals [13] based on speculation where film and material have not been distinguished.

One of the reasons that this new theory has not yet been accepted is that researchers are unwilling to accept that material is different from film. They consider a block of material making up a film to have the same properties as the material in general. However, while permittivity ε_r and permeability μ_r can be properties of material [16], scattering parameters such as reflection loss *RL* are parameters for devices and not for material [7, 8, 14, 16]. Film, which has thickness, is a device made of material but thickness obviously cannot be a general property of material. Similarly, *RL* can be the property of a specific block of material but it is not a general property of material. Thus, properties unique for the block cannot be attributed to the material. There is much evidence showing that many wrong theories in this field have been developed by overlooking this basic tenet [8, 14, 15].

IM was developed by confusing film and material. Although IM is widely used to "predict" the absorption behavior of different materials, comprehensive theoretical support has not yet been provided as shown by the recent statement: "the relationship between impedance matching and material parameters has not been accurately described so far" [17]. Similarly, no theoretical proof exists for the related quarter-wavelength theory (QWM) as shown by the recently published statement [18]: "In the research and applications on microwave absorption materials and electromagnetic absorbers, the quarter-wavelength model is widely used in describing the dependence of the reflection loss (*RL*) peak frequency on electromagnetic parameters and thickness, and in the preparation and design of microwave absorption materials. However, strict proof regarding this model based on transmission line theory is lacking. Moreover, a deviation between the absorption peaks obtained from the *RL* results and those from the quarter-wavelength model is observed in some materials, for which a universal and reasonable theoretical explanation is also lacking." Despite correctly emphasizing this crucial omission, these authors [17, 18] were unable to provide a suitable proof [15].

The IM theory is characterized by $|Z_{in}(x_1^-)| = |Z_0|$ [17] where Z_{in} is the input impedance of film and Z_0 is the characteristic impedance of open space. We have shown previously that the minima of $|RL(x_1^-)|$ cannot be correctly obtained using IM [7], a fact which can be readily confirmed using published

data. For example, considering data for the film of $Ni_{0.6}Zn_{0.4}Fe_2O_4$ with film thickness d = 1.8 mm [19], it is found that $|Z_{in}(x_1^-)|$ is much nearer to $|Z_0|$ in the frequency range from 7 – 18 GHz than when the material is replaced by its composites with different amounts of $SrFe_{12}O_{19}$. However, the relative values of $|RL(x_1^-)|$ for the films with different materials are quite different from those predicated by IM. Even though these results from the films of the compound and its composites contradict predictions from IM in the whole frequency range from 0.5 – 18 GHz, the data were still used to support IM [19]. It should be noted that in publications it is common practice to claim a correlation between IM of the film and the power absorption coefficient α_P of material [12, 20-22] but in fact, such correlation does not exist because film and material are different.

It will be further shown here that replacing the common criterion of IM by $|Z_{in}(x_1^-) = Z_0|$ [23, 24] cannot fix the problems. Even though the minima of $|RL(x_1^-)|$ can be correctly predicted by the phase difference of beams t and 1_r at $\phi = (2n + 1)\pi$ [7, 8], this condition cannot be taken to be equivalent to, and therefore replaced by the requirement that $Z_{in}(x_1^-)$ and Z_0 are in phase because the value of $RL(x_1^-)$ cannot always be predicted by $|Z_{in} - Z_0|$ while the effect of $|Z_{in} + Z_0|$ in the expression of $RL(x_1^-)$ is ignored [7]. In addition, ignoring the relevance of wave superposition in film has led to the development of the QWM which is flawed because a film contains interfaces whose phase effects are ignored [7, 15, 25]. The shortcomings in IM and the QWM have been

highlighted previously using rigorous theoretical arguments from transmission-line theory. Here those conclusions will be verified explicitly, from a different theoretical perspective shown in section 2.1, using experimental data obtained from films with a material not previously studied. The polar presentation used in section 2.7 is a novel persuasive vehicle.

It is sometimes argued that there are numerous sets of experimental data published that "support" the accepted theories [26] and by contrast that only a few examples have been provided for the new theory [7, 27]. For that reason, further experimental evidence needs to be accumulated and this work provides another example. Such analyses can be applied to all published data and by using our new theory based on wave superposition, it can be easily seen such data were inconsistent with the previously accepted theories. In history, wrong theories were always "supported" by experiments until the theories were proved wrong [28, 29]. Although only a few sets of data from various compounds have been used to support our conclusions [6, 7, 16, 27, 30], their variety and the principles used for the analyses suggest that all experimental data published previously in the literature will support our conclusions. The experimental supports provided in this work are convincing and the theoretical arguments are easily accessible by experimentalists since the theoretical background is not beyond college physics.

2. A quantitative verification of the theoretical results from experimental data

We have previously shown that the minima of $|RL(x_1^-)|$ can be described accurately using wave cancellation theory WCT [7, 8] and as a consequence, we qualitatively identified the flaws in the QWM [7, 15, 25]. Based on quantitative mathematics shown in section 2.1, here, we verify the results of WCT using our own experimental data obtained from the film of composite $BaFe_{11.8}Ce_{0.2}O_{19}$/polypyrene [31], as shown in Fig. 1 [32]. We would have preferred to use experimental data from other research groups. However, for our purpose, raw experimental data are required which are difficult to obtain being rarely available online. Nevertheless, the analysis presented are generally applicable.

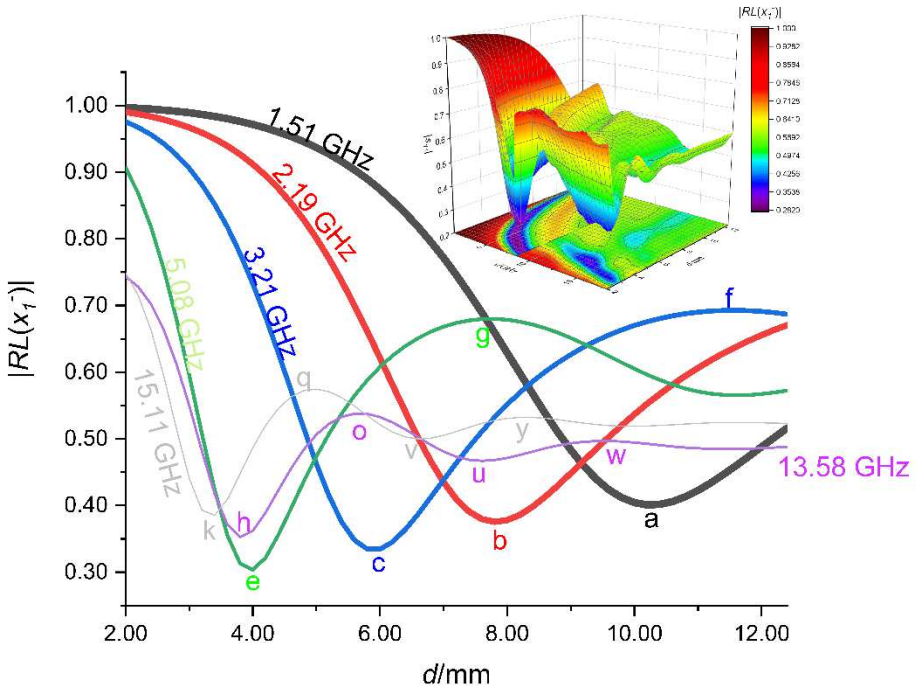

Fig. 1 The minima and maxima of $|s_{11}(d)|$ for MB at different values of ν indicated by letters a, b, c, etc. The two-dimensional curves of $|RL(x_1^-)|$-d were sampled at specific values of ν from the inset of the three-dimensional graph of $|RL(x_1^-)|$-ν-d for MB of composite $BaFe_{11.8}Ce_{0.2}O_{19}$/polypyrene synthesized in our laboratory. The measurements were conducted by a vector network analyzer (VNA)

using E85071C with Keysight Technologies 85055AR03-FG Airline Type N, 50 Ohm Replacement Kit. The film was prepared using a weight ratio of the composite to paraffin wax of 3:7 and was in a donut shape with inner and outer diameters of 3 and 7 mm respectively. The projection of $|RL(x_1^-)|$ from the inset shows the inverse relationship between d and ν for associated $|RL(x_1^-)|$ at different positions obtained by varying both d and ν. The values of RL (or s_{11}) are calculated from the measurements of ε_r and μ_r.

2.1 The effects specific to film revealed by mathematics

Principles behind the data illustrated in Figs. 1 – 4 can be revealed from fundamental principles in physics and related mathematical reasoning. First, the main effect represented by the $e^{-4j\pi\nu\frac{\sqrt{\varepsilon_r\mu_r}}{c}d}$ term in $|RL(x_1^-)|$ (Eq. A5 in Appendix A1) on forming its peaks will be discussed. The main factor responsible for the formation of peaks is the phase (angular) effect [8] represented by Eq. 1. ν is frequency; λ_M is the wavelength within film; and c is the speed of light in vacuum.

$$e^{-4j\pi\nu\frac{\sqrt{\varepsilon_r\mu_r}}{c}d} = e^{-\alpha_P d}e^{-j\alpha_j d} = e^{-\alpha_P d}e^{-4j\pi\frac{d}{\lambda_M}} \quad (1)$$

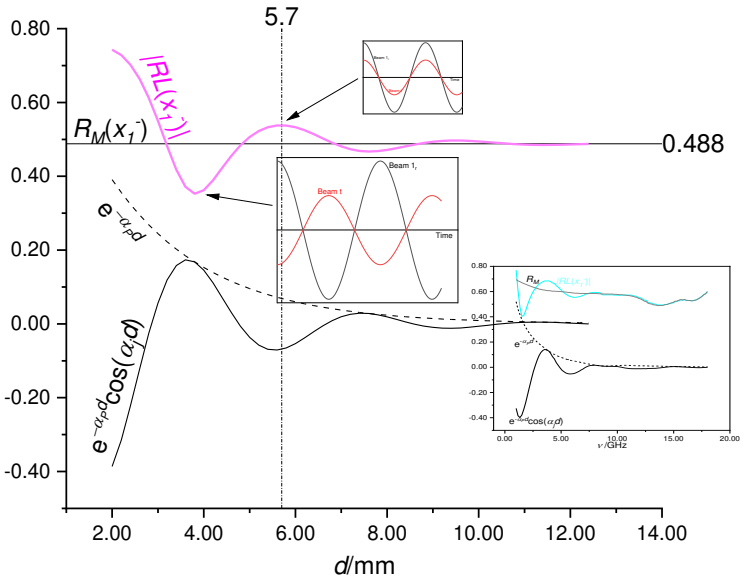

Fig. 2 The correlation between positions of the minima and maxima amplitudes of $|RL(x_1^-)|$ with beam 2_r (Eq. 3) at $\nu = 13.58$ GHz for the MB of $BaFe_{11.8}Ce_{0.2}O_{19}$/polypyrene. The curve of $|RL(x_1^-)|$ values is repeated from Fig. 1. The effect of Eq. 1 on the peak positions of $|RL(x_1^-)|$ is revealed by the curve of $\exp(-\alpha_P d)\cos(\alpha_j d)$. The arrows show that the maxima of $|RL(x_1^-)|$ are achieved if beams 1_r and t are in phase and the minima are achieved if they are out of phase by π. These parameters are presented in the insets with d = 10 mm and abscissa $\nu.|R_M|$ is 0.488, a value which is independent of d. $R_M(x_1^{--})$ is the reflection coefficient of the front interface of MB at x_1.

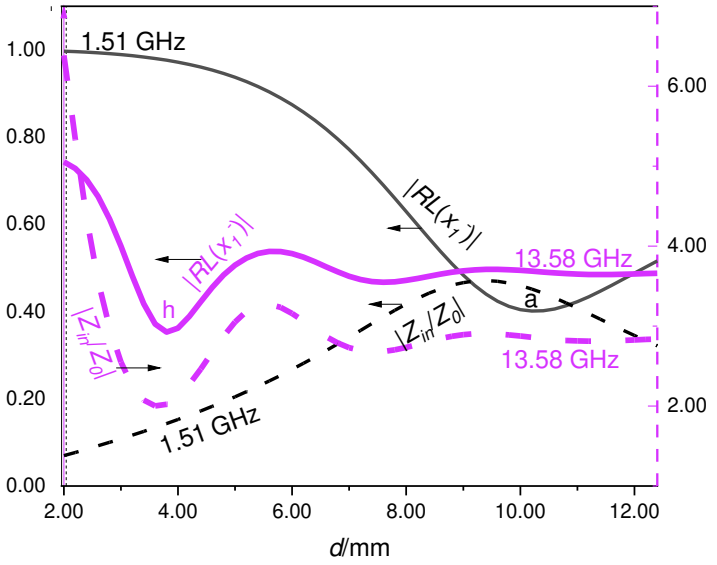

Fig. 3 A plot of $|Z_{in}/Z_0|$ (dashed lines) and $|RL(x_1^-)|$ (solid lines) at x_1^- in Fig. 1 versus d with frequency 1.51 (black) and 13.58 (purple) GHz for the MB film of $BaFe_{11.8}Ce_{0.2}O_{19}$/polypyrene. The arrows indicate which ordinate axis is used for the curve (only one points to the right). Labels a and h indicate the minimum peaks of $|RL(x_1^-)|$. $|RL(x_1^-)|$ curves are repeated from Fig. 1.

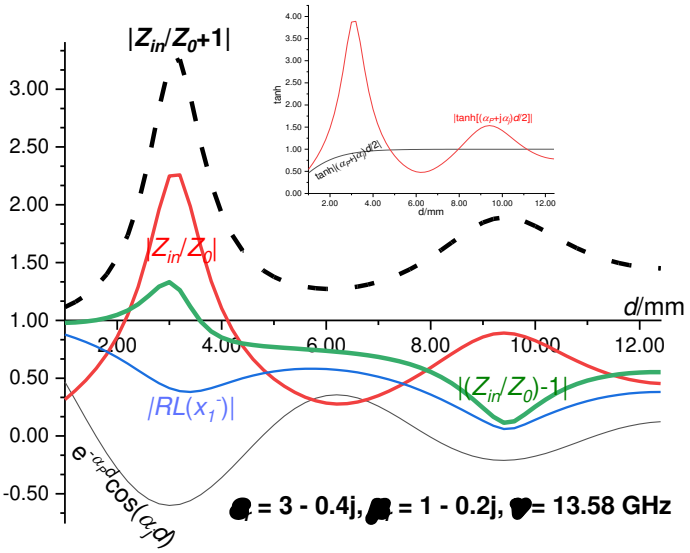

Fig. 4 Comparison of different criterions of IM and wave cancellation for the minima of $|RL(x_1^-)|$. Values for ε_r, μ_r and ν used for the calculations of $|RL(x_1^-)|$ and $|Z_{in}/Z_0|$ are indicated. The inset shows plots of tanh(y) and |tanh(y)| against d, $y = (\alpha_P + j\alpha_j)d$. The incorrect criteria used in developing IM have arisen from confusing real and complex numbers and neglecting the effect of $|Z_{in}/Z_0 + 1|$.

Considering the product $e^{-\alpha_P d}e^{-4j\pi\frac{d}{\lambda_M}}$ in Eq. 1, the term $e^{-\alpha_P d} = |e^{-\alpha_P d}e^{-4j\pi\frac{d}{\lambda_M}}|$ which is related to the attenuation of material, while the phase factor $e^{-4j\pi\frac{d}{\lambda_M}}$ is related to the angular effect specific for film [8] and is responsible for the peak formation of $|RL(x_1^-)|$ as shown in Figs. 2 and 4. The sine term of $e^{-4j\pi\frac{d}{\lambda_M}}$ vanishes when $\alpha_j d$ is a multiple of π or is very small when $\alpha_j d$ is close to being a multiple of π. Thus, the origin of the peak positions of $|RL(x_1^-)|$ can be illustrated by ignoring the imaginary part represented by the sine term. The measurable values for $|e^{-4j\pi\frac{d}{\lambda_M}}|$ fall between the limits of -1 and +1 which is consistent with Eq. 2.

$$Ae^{-\alpha_P d}\cos(\alpha_j d) = Ae^{-\alpha_P d}\cos(4\pi\frac{d}{\lambda_M}) \qquad (2)$$

The peak positions of $|RL(x_1^-)|$ are related to the phase effect represented by cos($\alpha_j d$) [7, 8, 15]. The effect of Eq. 2 on $RL(x_1^-)$ may be much larger than ±1 since complex numbers are involved in Eq. A5. The cos term in Eq. 2 can be used to predict that peaks a, b, c, and e in Fig. 1 occur at d =

$\lambda_M/4$, which is consistent with the QWM, and peaks h and k occur at $d = \lambda_M/2$, which do not conform since they [7, 25].

The results from Fig. 1 are summarized in Table 1. As shown by Figs. 2 and 4, the peaks of $|RL(x_1^-)|$ are formed when $|Z_{in}| \neq |Z_0|$, a fact which cannot be accounted for by IM where the phase of Z_{in} is not invoked.

Table 1 The quantities at the minima and maxima of $|s_{11}|$ for MB extracted from Fig. 1 for the film of composite $BaFe_{11.8}Ce_{0.2}O_{19}$/polypyrene. Frequency ν is in units of GHz, wavelength λ_M and film thickness d in mm. $|s_{11}|$ is the same as $|RL(x_1^-)|$.

ν	Z_M/Z_0	$d_{min}(1)$	$d_{min}(1)/\lambda_M$	$d_{max}(1)$	$d_{max}(1)/\lambda_M$	$d_{min}(2)$	$d_{min}(2)/\lambda_M$	$d_{max}(2)$	$d_{max}(2)/\lambda_M$
λ_M	R_M	exp(-$\alpha_f d$)	$\alpha_r d$	exp(-$\alpha_f d$)	$\alpha_r d$	exp(-$\alpha_f d$)	$\alpha_r d$	exp(-$\alpha_f d$)	$\alpha_r d$
		$\|s_{11}\|$(min)	$\alpha_f d$	$\|s_{11}\|$(max)	$\alpha_f d$	$\|s_{11}\|$(min)	$\alpha_f d$	$\|s_{11}\|$(max)	$\alpha_f d$
1.51	0.20+0.06j	10.25	0.26						
40.34	-0.67+0.09j	0.37	0.99						
		0.40	3.19						
2.19	0.22+0.07j	7.80	0.25						
30.69	-0.64+0.09j	0.36	1.03						
		0.38	3.19						
3.21	0.24+0.07j	5.90	0.26	11.60	0.500				
23.04	-0.61+0.10j	0.36	1.03	0.13	2.02				
		0.33	3.22	0.69	6.33				
5.08	0.25+0.08j	4.00	0.26	7.70	0.50	11.60	0.75		
15.39	-0.59+0.10j	0.36	1.03	0.14	1.98	0.05	2.98		
		0.30	3.27	0.68	6.29	0.57	9.47		
13.58	2.78-0.55j	3.80	0.50	5.70	0.75	7.80	1.02	9.50	1.25
7.62	0.48-0.08j	0.17	1.78	0.07	2.68	0.02	3.66	0.01	4.46
		0.35	6.27	0.53	9.40	0.47	12.86	0.50	15.66
15.11	3.02-0.67j	3.50	0.53	5.00	0.75	6.60	1.00	8.30	1.25
6.63	0.52-0.08j	0.16	1.82	0.07	2.61	0.03	3.44	0.01	4.33
		0.39	6.63	0.57	9.47	0.50	12.51	0.53	15.73

IM requires that beam t completely cancels beam 1_r if $Z_{in} = Z_0$. But it should be noted that $Z_{in} \neq Z_0$ for all the peaks of $|RL(x_1^-)|$ shown in Figs. 1 – 4. Only the phase condition based on Eq. 1 functioning as an angular effect

is responsible for peak formation [8]. The peaks are broad, since the condition that $|Z_{in} - Z_0| = 0$ [6] is not obligatory. As shown by Fig. 2, the monotonic function $e^{-\alpha_P d}$ in Eq. 2 is not a factor for the formation of $|RL(x_1^-)|$ peaks. Examples are presented in Figs. 3 and 4 showing that $|RL(x_1^-)|$ peaks do not occur at positions with the optimum IM specified by $|Z_{in}/Z_0| = 1$.

When $\alpha_P d$ is sufficiently large, the main beam among 2_r, 3_r, 4_r, etc. in beam t is beam 2_r which is demonstrated by Eq. 3 for MB

$$
\begin{aligned}
&V(\mathrm{t}, x_1^-) = V(2_\mathrm{r}, x_1^-) + V(3_\mathrm{r}, x_1^-) + V(4_\mathrm{r}, x_1^-) + \ldots + \\
&= -V(\mathrm{i}, x_1^-) \frac{[1 - R_M^2(x_1^-)] e^{-4j\pi\nu \frac{\sqrt{\varepsilon_r \mu_r}}{c} d}}{1 - R_M(x_1^-) e^{-4j\pi\nu \frac{\sqrt{\varepsilon_r \mu_r}}{c} d}} \\
&= -V(\mathrm{i}, x_1^-)[1 - R_M^2(x_1^-)] e^{-4j\pi\nu \frac{\sqrt{\varepsilon_r \mu_r}}{c} d} [1 \\
&+ R_M(x_1^-) e^{-4j\pi\nu \frac{\sqrt{\varepsilon_r \mu_r}}{c} d} + R_M^2(x_1^-)] e^{-8j\pi\nu \frac{\sqrt{\varepsilon_r \mu_r}}{c} d} + \ldots] \\
&\approx -V(\mathrm{i}, x_1^-)[1 - R_M^2(x_1^-)] e^{-4j\pi\nu \frac{\sqrt{\varepsilon_r \mu_r}}{c} d} = V(2_\mathrm{r}, x_1^-) \\
&= A e^{-\alpha_P d} e^{-4j\pi \frac{d}{\lambda_M}}
\end{aligned}
\qquad (3)
$$

where for fixed ν, A is a constant with respect to d. $V(\mathrm{k}, x)$ is the voltage of beam k at x. Equation 3 describes the amplitude effect [7] of film and is responsible for the deformed spiral shape of the $|V(\mathrm{t}, x_1^-)|$ curve plotted with respect to $\alpha_f d$ in the polar coordinate system. From Eq. 3, beams t and 1_r are out of phase by π if $d = \lambda_M/4$ when $Z_M < Z_0$ and if $d = \lambda_M/2$ when $Z_M > Z_0$. The results conform to the inverse relationship needed to replace QWM [7, 15, 25, 33]. If $\alpha_P d$ is small, beams 3_r, 4_r, 5_r, etc. cannot be neglected and thus the denominator in Eq. 3 might make $|V(\mathrm{t}, x_1^-)| > |V(\mathrm{i}, x_1^-)|$ [8, 14].

Equation 3 also shows that Eq. 1 or 2 are only approximate for the case where $Z_{in} \neq Z_0$ since they only account for beam 2_r, which is the main beam in beam t. Even in Eq. 3, the imaginary part of R_M in A will cause the minimum position of $|RL(x_1^-)|$ to deviate from that predicted by the $e^{-4j\pi\frac{d}{\lambda_M}}$ term. As shown by Figs. 2 and 4, the minima of $|RL(x_1^-)|$ do not occur exactly at positions predicted by $\cos(4\pi\frac{d}{\lambda_M})$ in Eq. 2 since a small additional phase from the imaginary parts of R_M and $1-R_M(x_1^-)e^{-4j\pi\nu\frac{\sqrt{\varepsilon_r\mu_r}}{c}d}$ in $RL(x_1^-)$ also contributes to peak formation which confirms the fact that peaks a, b, c and e in Fig. 1 do not occur exactly at $d = \lambda_M/4$ as predicted by the QWM and by IM.

The angular effect [8] is demonstrated by Eqs. 2 and 3. The minimum peaks of $|RL(x_1^-)|$ are achieved when beams 1_r and t are out of phase at $\phi = (2n + 1)\pi$ and the maximum peaks are achieved when the two beams are in phase at $\phi = 2n\pi$ where ϕ is the phase difference of the two beams. $|RL(x_1^-)|$ is determined by energy conservation specific to film, since its value is related to the amplitude of the resultant beam from 1_r and t [8, 14]. When $\phi = (2n + 1)\pi$, more back-and-forth reflections in the film are necessary to return the required microwave energy to open space since beam 1_r should be canceled by beam t. It should be noted that the energy returning to the open

space from the film cannot be calculated from the respective squared amplitudes of beams 1_r and t, a mistake commonly made [34, 35].

Thus, as required by energy conservation, the amplitude of beam t reaches its maxima when the minima of $|RL(x_1^-)|$ are attained, a result contrary to the common belief that maximum absorption occurs when beam t is the weakest possible [13]. This wrong belief is the basis for the argument that the most efficient absorption represented by *RL*/dB can be achieved by increasing the dispatching power of material and the amount of microwaves that penetrates the film [36-41]. However, such arguments are invalid because they confuse film with material. For film, beam 1_r is in phase with beam t at $\phi = 2n\pi$. Thus, to return the required energy by energy conservation, a weak beam t is sufficient since beam 1_r is in phase with beam t. When $\phi = (2n + 1)\pi$, beam t is canceled by beam 1_r. To return the required energy to the open space, beam t must be stronger which is achieved by increasing the amount of back-and-forth reflections in the film [8, 14]. For a film that does not dispatch microwaves, any number of reflections will not enable absorption, and the number of reflections in film is determined by energy conservation. For an absorbing film, the number of reflections in the film is also related to absorption efficiency.

2.2 Verification of the new theory from experimental data

For MB made from $BaFe_{11.8}Ce_{0.2}O_{19}$/polypyrene, beam 1_r is out of phase with beam i at x_1^- by approximately π for frequencies below 8.48 GHz, as shown by the values of $R_M(x_1^-)$ or Z_M/Z_0 in Table 1 for the frequencies of 1.51, 2.19, 3.21, and 5.08 GHz and the small value of the imaginary part of $R_M(x_1^-)$ does not result in a significant deviation from a phase difference of π. This relationship between beams 1_r and i is validated by the reflection coefficient of the front interface at x_1 and can be simplified if the imaginary part of $R_M(x_1^-)$ is ignored.

The first minimum of $|RL(x_1^-)|$ for each of the frequencies 1.51, 2.19, 3.21, and 5.08 GHz (Fig. 1) occurs at film thicknesses [indicated by $d_{min}(1)$ in Table 1] of 10.25, 7.80, 5.90, and 4.00 mm, respectively. As indicated in the fourth column of Table 1, these values of $d_{min}(1)$ are close to, but not equal to, $\lambda_M/4$ of the microwaves at their respective frequencies. It should be noted therefore that these values are only accurate to 2 figures of decimals.

For each of the peaks a, b, c, and e, in order to obtain a minimum peak of $|RL(x_1^-)|$, it is necessary for beam t or the sum of beams 2_r, 3_r, 4_r, etc. to be out of phase by π with beam 1_r. In other words, $\cos(4\pi \frac{d}{\lambda_M}) = -1$ when $d = \lambda_M/4$. Since A in Eq. 3 is negative, then $V(t, x_1^-)$ and $V(i, x_1^-)$ will have the same sign when $Z_M < Z_0$. Thus, in MB a minimum peak of $|s_{11}|$ (or $|RL(x_1^-)|$) is formed since beams t and 1_r are out of phase by π where both $e^{-4j\pi\nu\frac{\sqrt{\varepsilon_r\mu_r}}{c}d}$ and $R_M(x_1^-)$ in the formula for RL given in Eq. A5 have the same sign but

different values. The same analysis applies to the second minimum of $|RL(x_1^-)|$ when $d = 3\lambda_M/4$ as indicated by columns 7 and 8 in Table 1 for the curve of frequency 5.08 GHz in Fig. 1 where $d_{min}(2)$ = 11.6 mm. The first maximum for curves of frequencies 3.21 and 5.08 GHz occurs at $d_{max}(1)$ = 11.6 and 7.7 mm, respectively, where $d = \lambda_M/2$. Here, the resultant beam from beams 2_r, 3_r, 4_r, etc. is in phase with beam 1_r so that $|RL(x_1^-)|$ achieves its maximum value. From Eq. 2, $\cos(4\pi \frac{d}{\lambda_M}) = 1$ when $d = \lambda_M/2$. $V(t, x_1^-)$ and $V(i, x_1^-)$ have opposite signs which ensures a maximum for $|RL(x_1^-)|$ since beams t and 1_r are then in phase.

2.3 The precise positions of the peaks of $|RL(x_1^-)|$

As shown by the verifications, the principle introduced in section 2.1 has identified the main factor that determines the peak positions of $|RL(x_1^-)|$. However, it must be said that there are other factors which cause these peak positions to deviate from those predicated by Eq. 2. The vertical line at d = 5.7 mm in Fig. 2 shows the deviation of the phase correlation between peak positions of $|RL(x_1^-)|$ and $\cos(\alpha_j d)$ which occurs because the phase difference between beams t and 1_r in Fig. 1 cannot be exactly defined by $\cos(\alpha_j d)$. This is because the minimum position of $|RL(x_1^-)|$ is not only affected by beam 2_r characterized in Eq. 3, but also by the terms in the formula for $RL(x_1^-)$, namely $R_M(x_1^-)$ in the numerator and $1 - R_M(x_1^-)e^{-4j\pi\nu\frac{\sqrt{\varepsilon_r\mu_r}}{c}d}$ in the denominator as they are

both complex numbers and their imaginary parts make a small contribution. $R_M(x_1^-)$ is related to beam 1_r and $1-R_M(x_1^-)e^{-4j\pi\nu\frac{\sqrt{\varepsilon_r\mu_r}}{c}d}$ is related to the sum of the individual beams in t.

The minima positions of $|RL(x_1^-)|$ deviate slightly from $d = \lambda_M/4$ but these deviations are necessary to keep the phase difference between beams t and 1_r at π. Two effects contribute to the deviations. The small imaginary part of $R_M(x_1^-)$ contributes to the numerator in $RL(x_1^-)$ which affects the phase of beam 1_r directly. The second effect emanates from the small imaginary part of the denominator of $|RL(x_1^-)|$ which is a cumulative effect from $R_M(x_1^+)$ for beams 2_f, 3_f, etc., and from Z_M in the transmission coefficients $\gamma(x_1^+)$ which includes the effect of $\gamma(x_1^+)$ on beam 1_f and the effect of $\gamma(x_1^-)$ on beams 2_r, 3_r, 4_r, etc. All these factors affect the phase of beam t. Thus, to ensure that the phase difference between beams 1_r and t is π, d needs to be adjusted so that the phases of the two beams are shifted as required by the two effects.

The requirement that the phase difference between beams 1_r and t is $(2n + 1)\pi$ for the minima of $|RL|$ is only a first approximation. In fact, the above effects will produce minima of $|RL|$ that do not occur exactly at either $d = (2n + 1)\lambda_M/4$ or $n\lambda_M/2$, or $\phi = (2n + 1)\pi$. The shifts in these positions can be understood from the absorption mechanism of film by considering the balance between the angular effect of film represented by $\alpha_f d$ and the attenuation effect of material represented by $\alpha_P d$ [8]. Results revealed by this balance are that the maxima of

$|R_2|$ and $|RL|$ occur at $\phi < (2n + 1)\pi$ and $\phi < 2n\pi$, respectively, while their minima occur at $\phi > 2n\pi$ and $\phi > (2n + 1)\pi$, respectively, if ε_r'' and μ_r'' are not too large. $R_2(x_1^-) = V(\mathrm{t}, x_1^-)/V(\mathrm{i}, x_1^-)$. It can also be proved that the shifts in these maximum positions are larger than in their corresponding minimum positions. It should be noted that the amplitudes of individual beams also affect the phase of the resultant beam in wave superposition and this effect shifts the maximum and minimum positions of |t| and $|RL|$ from $\phi = n\pi$. This effect of amplitude has already been included in the derivation of the formula of *RL*.

2.4 The inverse relationship between frequency and film thickness

It has been proposed that the theory of QWM is valid in all circumstances but it has been shown that it cannot be applied to magnetic materials at high frequencies because then the minima of $|RL(x_1^-)|$ occur at $d = n\lambda_M/2$ instead of $(2n + 1)\lambda_M/4$ [7, 25]. Using data from $BaFe_{11.8}Ce_{0.2}O_{19}$/polypyrene in MB, beam 1_r is approximately in phase with beam i at x_1^- for frequencies higher than 8.65 GHz (the step $\Delta\nu$ used in the measurement is 170 MHz), as exemplified by the values of $R_M(x_1^-)$ or Z_M/Z_0 in Table 1 for frequencies of 13.58 and 15.11 GHz. In such a case, beam t needs to be out of phase with 1_r by π to minimize $|RL(x_1^-)|$ when *d* is approximately $\lambda_M/2$ and in phase to maximize $|RL(x_1^-)|$ when *d* is approximately $3\lambda_M/4$. These results can also be verified from Eq. 2 and are illustrated in Fig. 1 and Table

1 with data from frequencies of 13.58 and 15.11 GHz. These quantitative results cannot be explained by the QWM.

Peak a for the curve with ν = 1.51 GHz in Fig. 1 is achieved at d = 10.25 mm with νd = 15.48 (mm·GHz). The value of $\alpha_j d$ (rad) in Eq. 2 for this peak is 3.19 ($\approx \pi$) and keeps its value in peak b where d is reduced to 7.80 mm and ν is increased to 2.19 GHz where νd = 17.10. The small difference between the values of νd occurs because ε_r and μ_r are functions of frequency. As indicated by Table 1, the values of $\alpha_j d$ are also approximately the same for peaks a, b, c, and e, and equal to ~2π for peaks f and g. Similarly results from high-frequency curves given in Table 1 show that pairs, (h, k), (o, q), (u, v), and (w, y) have similar values of $\alpha_j d$ [15] . The correlation between the phases of $|RL(x_1^-)|$ and $\cos(\alpha_j d)$ is shown in Fig. 2.

As shown in Table 1, the values of $\exp(-\alpha_P d)$ are approximately the same for different peaks of each group, e.g. (a, b, c and e); (f and g); (h and k); (o and q), (u and v) and (w and y) in Fig. 1. Therefore, the inverse relationship [15, 30, 33] between d and ν for $|RL(x_1^-)|$ is indicated from the projection of $|RL(x_1^-)|$ on the ν - d plane in the inset of Fig. 1 and thus in this specific case there is some validity for the discredited QWM when $\sqrt{\varepsilon_r \mu_r}$ can be considered as a constant when $Z_M < Z_0$ for MB. Contrary to the claim in the QWM, it can be said that an inverse relationship exists between d and ν for a series of related minima of $|RL(x_1^-)|$, and the relationship does indeed exist for a series of related $|RL(x_1^-)|$

with the same value of $(\alpha_P + j\alpha_j)d$. But this inverse relationship is not only valid for the minima of $|RL(x_1^-)|$ since it can also be applied to the maxima [15].

If the values of R_M and $\sqrt{\varepsilon_r \mu_r}$ are somewhat insensitive to frequency, then $|RL(x_1^-)|$ as well as Z_{in} should have the same value on an inverse curve of d and v. Indeed, such a curve with the same value of $|RL(x_1^-)| = 0$ will then be possible. However, the minima of $|RL(x_1^-)|$ reported in the literature on the inverse curve have different values even when $(\alpha_P + j\alpha_j)d$ is approximately constant. As shown from Table 1, $\alpha_j d$ as well as $\alpha_P d$ is approximately constant for peaks a, b, c, e in Fig. 1 which become successively stronger from peaks a to e, even though values of $\alpha_P d$ do not differ significantly. The fact that peaks on a reverse curve have different values is commonly reported in the literature. This is because ε_r, μ_r, and R_M cannot take the same value at different frequencies. $\alpha_j d$ determines the phase and peak formation for the $|RL(x_1^-)|$ which oscillates asymmetrically around $|R_M|$. The magnitude of the oscillation becomes smaller when the values of $\alpha_P d$ and $\alpha_j d$ increase and $|RL(x_1^-)|$ converges to $|R_M|$. At high frequency, α_P is relatively large, and thus the values of R_M have a greater influence on the peak values of RL/dB. The value of $|R_M|$ at frequency 13.58 GHz in Fig. 1 is smaller than that at frequency 15.11 GHz, thus the values of the h, o, u, w peaks on the curve with frequency 13.58 GHz are smaller than their counterparts with frequency 15.11 GHz.

Peaks a – e occur on the same reverse curve in Fig. 1 and the values of both $\alpha_P d$ and $\alpha_j d$ change little from peak to peak (Table 1). Thus, the amplitudes of the oscillations of $|RL(x_1^-)|$ have similar peak values at all four frequencies. The values of R_M become less negative (Table 1) but their peak values become progressively smaller since the amplitude of beam t is changed. Thus, at lower frequency, the peak values will be influenced more by the value of $\alpha_j d$, or by the angular effect.

The QWM should be based on the inverse relationship between d and ν for the minimum values of $|RL(x_1^-)|$, but this inverse relationship can be generally valid for any value of $|RL(x_1^-)|$ with constant $\alpha_P d$ and $\alpha_j d$.

2.5 The flaws in the impedance matching theory

In current theory, all minima of $|RL(x_1^-)|$ have been attributed [9, 42-49] to the effects of IM, even though there is only one minimum position defined by IM, which occurs when $Z_{in} = Z_0$. However, the peak determined by $Z_{in}(x_1^-) = Z_0$ is very narrow [6] and thus wider peaks cannot be attributed to that equality. The reported peaks do not represent the narrow peaks at $Z_{in}(x_1^-) = Z_0$ but rather are the wide peaks caused by WCT at $Z_{in}(x_1^-) \neq Z_0$ [7, 8], which suggests that the narrow peak has not been detected either because the frequency step used is too large or it does not exist at all because the amplitude and phase conditions required by $Z_{in}(x_1^-) = Z_0$ cannot be satisfied simultaneously. Indeed, it cannot be demonstrated using IM why the reported peaks do not occur exactly at $|Z_{in}(x_1^-)| = |Z_0|$ or at $Z_{in}(x_1^-) = Z_0$. This

inconsistency between the data and IM apparent in published reports has not been remarked upon in the literature, presumably because of a lack of theoretical knowledge. What is more, there are many valleys illustrated in the inset in Fig. 1 and each represents a group of minima of $|RL(x_1^-)|$. At most, there is only one group of minima that meets the condition that $Z_{in}(x_1^-) = Z_0$, while for all other groups, the values of $|Z_{in}(x_1^-)|$ are far removed from that of $|Z_0|$.

It should also be noted that the $|RL(x_1^-)|$ peak at $Z_{in}(x_1^-) = Z_0$ is different from peaks occurring where $|Z_{in}(x_1^-)| \neq |Z_0|$. Contrary to common belief, the minimum values of $|RL(x_1^-)|$ are not determined by how close $|Z_{in}(x_1^-)|$ is to $|Z_0|$ as it can be seen from Fig. 4 that intense peaks can be achieved at positions where the difference is significant [7]. For example, the positions of peaks a and h at ν = 1.51, 13.58 GHz respectively in Fig. 3 do not occur where $|Z_{in}/Z_0|$ is closest to 1. Furthermore, peak h is stronger than peak a, but occurs at a position where $|Z_{in}/Z_0|$ deviates significantly more from 1. The minimum value of $|RL(x_1^-)|$ is not just determined by the condition $|Z_{in}(x_1^-)| = |Z_0|$ as its value is also affected by the phase of $Z_{in}(x_1^-)$ in $|Z_{in}(x_1^-) - Z_0|$, and as shown in Fig. 4, the effect of $Z_{in}(x_1^-) + Z_0$ on $|RL(x_1^-)|$ cannot be neglected.

It should be noted that $Z_{in}(x_1^-)$ is a complex number so that the values of $Z_{in}(x_1^-) - Z_0$ and $|Z_{in}(x_1^-)| - |Z_0|$ are not the same. $|Z_{in}|$ is a function of ν and a periodic function of $\alpha_j d$ and the curves of $|Z_{in}/Z_0|$ are shown by Figs. 3 and 4. In current theory, the peak values of $|RL(x_1^-)|$ have often been related to

$|Z_{in}/Z_0|$ or $|Z_{in}/Z_0 - 1|$ without precise numerical proof. Even when numerical values were calculated, the evidence contrary to IM was still claimed as providing support for it [10, 43-45, 50]. The correlation between the peak values of $|RL(x_1^-)|$ and IM is not valid as shown by Figs. 3 and 4, and only WCT can provide the correct results [7, 8]. The effect of phase on peak formation also affects peak value. Thus, the value and width of the $|RL(x_1^-)|$ peak [51] cannot be attributed to IM, since the peak is caused by the phase differences described in WCT.

At 3.21 GHz, $\varepsilon_r = 13.97 - 9.78j$ and $\mu_r = 1.06 - 0.01j$. As shown in Table 1, the characteristic impedance of the material Z_M/Z_0 is $0.24 + 0.07j$, $Z_M \neq Z_0$, and the reflection coefficient of the interface at x_1 $R_M(x_1^-)$ is $- 0.61 + 0.10j$. From the real part [14] of

$$R_M^2(x_1^-) = \left[\frac{Z_M - Z_0}{Z_M + Z_0}\right]^2 \qquad (4)$$

it can be calculated that 36.2% of the incident energy has been reflected from the interface in its isolated state, and from the transmitted coefficient $\gamma_M(x_1^+)$ or the real part [14] of

$$\frac{Z_0}{Z_M}\gamma_M^2(x_1^+) = \frac{Z_0}{Z_M}\left[\frac{2Z_M}{Z_M + Z_0}\right]^2 \qquad (5)$$

That 63.8% of the incident energy has penetrated the interface in its isolated state [14]. Since IM has not differentiated between interfaces in its isolated state and in film, it is assumed [52, 53] that the same amount of

microwaves penetrates films with different d represented by the curve of 3.21 GHz in Fig. 1. Thus, it is clear that IM cannot explain why different absorptions occur at the same amount of penetration.

Since $RL(x_1^-) = 0.3332$ for the MB with $d = 5.90$ mm and $\nu = 3.21$ GHz as shown in Fig. 1, $1 - RL(x_1^-)^2 = 88.90\%$ of the incident energy has been absorbed by the film. This is a natural result from transmission-line theory. However, IM cannot explain this result since 88.90% of the incident energy has been absorbed while only 63.8% of the incident energy entered the material. The explanation for this result given by IM is convoluted in that it seems to be that the energy reflected by beam 1_r has been retaken into the film by the back-and-forth reflections within the film. But this is unreasonable since the energy entering the film cannot be defined by the amplitude of the beam penetrating the interface. The properties of the interface in film are different from those in its isolated state. By energy conservation, the energy entering MB is the amount absorbed by the film and that returned to the open space by beam t. However, the energy returned by beam t cannot be determined and thus the energy entering the film cannot be defined for film. By differentiating between the interfaces in its isolated state and film, this amount of absorption can be successfully explained via WCT bythe cancellation of beams 1_r and t, involving energy conservation for film.

The above results for the differences between film and material, and between interfaces in film and its isolated state, are considered surprising by

many experimentalists from a superficial understanding of energy conservation. However, the results are consistently obtained from experimental data using formulae that are generally accepted in both old and new theories. The evidence is beyond dispute, otherwise, the wave superposition theory and the fundamental formulae from transmission-line theory would be both wrong. The simple explanation is that the absorption mechanism for film is different from that of material though there might be additional reasons arising from quantum theory.

When the same portion of the above material with the same thickness d = 5.90 mm forms a film without metal-back (WMB), $|s_{11}| = 0.7425$ and $|s_{21}| = 0.3441$. This WMB absorbs $1 - |s_{11}^2| - |s_{21}^2| = 1 - 0.5513 - 0.1184 = 33.03\%$ of the incident energy while, as shown above, a MB absorbs 88.90% thus showing that these two devices have different properties [14]. It also provides clear evidence that RL and s_{11} are properties of devices and that material and films (devices) are different.

2.6 Examples related to impedance matching and quarter-wavelength theories

From the absorption mechanism involving WCT, it can be seen that $|RL(x_1^-)|$ is the correct parameter to use for characterizing microwave absorption for metal-backed film since only a small amount of microwave energy has been leaked out of the film if $|RL(x_1^-)|$ is a minimum. The remaining energy has been absorbed by the film. However, it is wrong to use $|RL(x_1^-)|$ to characterize material as its value is dependent upon the thickness

of the film d which is not a property of a material. When $Z_{in} = Z_0$, beam 1_r is still present since this condition for absorption is not the same as the condition $Z_M = Z_0$ for penetration [30], a fact which shows that while all microwaves have been absorbed, not all have penetrated the material [14]. This fact shows the flaws in IM that arise from confusing material and film. Thus, the fact that all the microwaves are consumed by the film when $Z_{in} = Z_0$ cannot be used to explain why the minima of $|RL|$ occur at $Z_{in} \neq Z_0$.

The errors in IM arise not only from the fact that the phase effect of Z_{in} has been ignored but also because both the criteria of $|Z_{in}|$ approaching $|Z_0|$ and of Z_{in} approaching Z_0 for the minima of $|RL|$ are wrong because to calculate the minima of $|RL(x_1^-)|$ when $Z_{in} \neq Z_0$, the effect of $|Z_{in} + Z_0|$ should not be neglected and $|Z_{in}|$ must be considered as a periodic function other than a constant.

The criterion that $|(Z_{in}/Z_0) - 1| = 0$ is based on the expression for $|RL(x_1^-)|$ which shows that $|RL(x_1^-)| = 0$ when $Z_{in} = Z_0$. But this does not signify that the condition $Z_{in} = Z_0$ can be achieved at $d = (2n + 1)\lambda_M/4$ as claimed by the QWM. For example, when the imaginary parts of ε_r and μ_r are both zero, we $RL(x_1^-)$ is a constant of 1 [7]. $|RL(x_1^-)|$ is monotonic decay function of d at fixed ν when $\varepsilon_r = \mu_r$. Both QWM and IM fail in these cases of $\psi_1 = 0$ since there is no absorption peak at all. Zhang et al [18] proposed a "strict proof" of the QWM based on the phase angle ψ_1 of Z_M, i.e., based on the formula for $|Z_{in}(x_1^-)|$ with the condition that $\psi_1 = 0$. However, it is illogical to apply

the result from $|Z_{in}(x_1^-)|$ to the minimum positions of $|RL(x_1^-)|$. What is important is that $\psi_1 = 0$ can be achieved only when the imaginary or real parts of both ε_r" and μ_r" are zero, or $\varepsilon_r = k\mu_r$. The flaw in the proof is exemplified above where there is no minimum of $|RL(x_1^-)|$ at $d = (2n + 1)\lambda/4$ when $\psi_1 = 0$ [7, 15]. It can be proved that the minima of $|RL(x_1^-)|$ do not occur exactly at $d = (2n + 1)\lambda_M/4$ or $n\lambda_M/2$ when $k \neq 1$ when ε_r and μ_r are complex.

A formula (Eq. 9 in the paper [18]) for the deviation of the minimum positions of $|RL(x_1^-)|$ from $d = (2n + 1)\lambda_M/4$ was obtained from Eq. 4c in that paper [18] involving the condition that $\psi_1 \neq 0$. However, while Eq. 4c provides a formula for the phase angle of $Z_{in}(x_1^-)$ it has been shown previously [15] that the derivation of that Eq. 9 is wrong.

It has proved incorrect to define IM for the minima of $|RL|$ in terms of the difference between $|Z_{in}(x_1^-)|$ and $|Z_0|$. As a result, two different criteria have been proposed [23, 24] with either $|Z_{in} - Z_0|$ or $|Z_{in}| - |Z_0|$ approaching 0 but neither solution is satisfactory. As shown by Fig. 3, $|RL(x_1^-)|$ achieves its minima around the minimum positions of $|Z_{in}(x_1^-)|$ when $|Z_M| > |Z_0|$ and around the maximum positions of $|Z_{in}(x_1^-)|$ when $|Z_M| < |Z_0|$ [7]. Thus, when $|Z_M| < |Z_0|$, as shown by Fig. 4, $|RL(x_1^-)|$ is a minimum near the maximum position of $|Z_{in}(x_1^-)|$, where $|Z_{in}(x_1^-) - Z_0|$ achieves its maximum value when $|Z_{in}(x_1^-)| > |Z_0|$ and its minimum when $|Z_{in}(x_1^-)| < |Z_0|$.

Thus, the first minimum $|RL(x_1^-)|$ peak in Fig. 4 shows that the problems of IM cannot be solved if it is defined by $|Z_{in}(x_1^-) - Z_0|$ and it cannot ensure a minimum $|RL(x_1^-)|$ peak even if $Z_{in}(x_1^-)$ and Z_0 are in phase. Z_{in} is complex and so is a periodic function related to the phase angle $\alpha_j d$ and the term $|Z_{in} + Z_0|$ cannot be neglected when calculating $|RL(x_1^-)|$. Thus the true condition for the minima $|RL(x_1^-)|$ is that beams 1_r and t are out of phase by π and not that $Z_{in}(x_1^-)$ and Z_0 are in phase.

All these problems with IM have been caused by assuming that the relevant parameters are real rather than complex [7]. Thus the periodicity of $|Z_{in}|$ has not been explicitly dealt with since its phase has not been considered and the term $|Z_{in} + Z_0|$ in the equation for $|RL(x_1^-)|$ has been ignored. As pointed out previously [15] $|Z_{in}|$ was wrongly taken to be a constant in the proof of the QWM [18]. The problems can be further identified from Fig. 4 which clearly shows that $|Z_{in}/Z_0| = 1$ at $d = 2.20$ and 4.20 mm, but that $|(Z_{in}/Z_0) - 1|$ and $|RL(x_1^-)|$ are not zero at those positions. Indeed, $|(Z_{in}/Z_0) - 1|$ is a maximum with a value far larger than zero at d = 3.2 mm. But near this position $|RL(x_1^-)|$ achieves its local minimum. The criterion of IM fails here because the effect of $|(Z_{in}/Z_0) + 1|$ has been neglected [7]. $|RL(x_1^-)|$ has achieved its minimum because $|(Z_{in}/Z_0) + 1|$ is larger than $|(Z_{in}/Z_0) - 1|$. However, WCT correctly predicts the positions of the minima of $|RL(x_1^-)|$ by applying the minima (in Fig. 4 for $Z_M < Z_0$) and the maxima (in Fig. 2 for $Z_M > Z_0$) of $\exp(-\alpha_P d)\cos(\alpha_j d)$.

The difference between analyses involving real and complex numbers is apparent in the inset in Fig. 4 which shows that $\tanh|(\alpha_P + j\alpha_j)d/2|$ is different from $|\tanh[(\alpha_P + j\alpha_j)d/2]|$ as the latter oscillates around 1 and approaches it when $\alpha_P d$ is large. Its maximum amplitudes are greater than 1 and its minima are less than 1. Its maxima and minima occur at $d = m\lambda_M/4$ and $d = n\lambda_M/2$ respectively, as indeed do values of $|Z_{in}|$. For MB, when $Z_M > Z_0$, the minima of $|RL(x_1^-)|$ occur near the positions of the minima of $|\tanh[(\alpha_P + j\alpha_j)d/2]|$, but when $Z_M < Z_0$, they occur near the positions at its maxima.

In IM it is assumed that Z_{in} is a monotonic real function of d or ν. However, this is only true when $(\alpha_P + j\alpha_j)d/2$ in the $\tanh[(\alpha_P + j\alpha_j)d/2]$ term is real. In such a case there is only one infinite minimum for *RL*/dB which occurs when $Z_{in} = Z_0$ where the effect of $Z_{in} + Z_0$ can indeed be neglected. When $(\alpha_P + j\alpha_j)d/2$ is complex, then the logic of IM fails since Z_{in} is complex and thus a periodic function, and as a consequence *RL*/dB can have multi-absorption peaks at $Z_{in} \neq Z_0$ and because of the effect of $Z_{in} + Z_0$, the minima of *RL*/dB can occur when Z_{in} deviates the most from Z_0. In Fig. 4, $|RL(x_1^-)|$ reaches its minima when $|Z_{in}(x_1^-)|$ reaches its maxima, approximately, where $|Z_{in}(x_1^-) - Z_0|$ are maximum when $|Z_{in}(x_1^-)| > |Z_0|$ and minimum when $|Z_{in}(x_1^-)| < |Z_0|$. This is the reason that the criterion of IM fails for the first $|RL(x_1^-)|$ minimum in Fig. 4.

2.7 An example presented by the polar coordinate system

Figure 4 shows an example where the minimum of *RL*/dB is achieved when Z_{in} deviates significantly from Z_0 and this has been attributed to the effect of $|Z_{in} + Z_0|$ on the value of *RL* [7]. If the value of Z_{in} is much larger than Z_0 when beams 1_r and t are out of phase by $\phi = (2n + 1)\pi$, then the minima of *RL*/dB can be achieved at a large difference between Z_{in} and Z_0. Such cases can be achieved under three conditions, namely that $\alpha_j d$ is relatively small, while $Z_M < Z_0$, and $|R_M|$ has a significant value. Alternatively, these three conditions are equivalent to a large $|R_2|$ shown by Fig. 5 for the case with $Z_M < Z_0$.

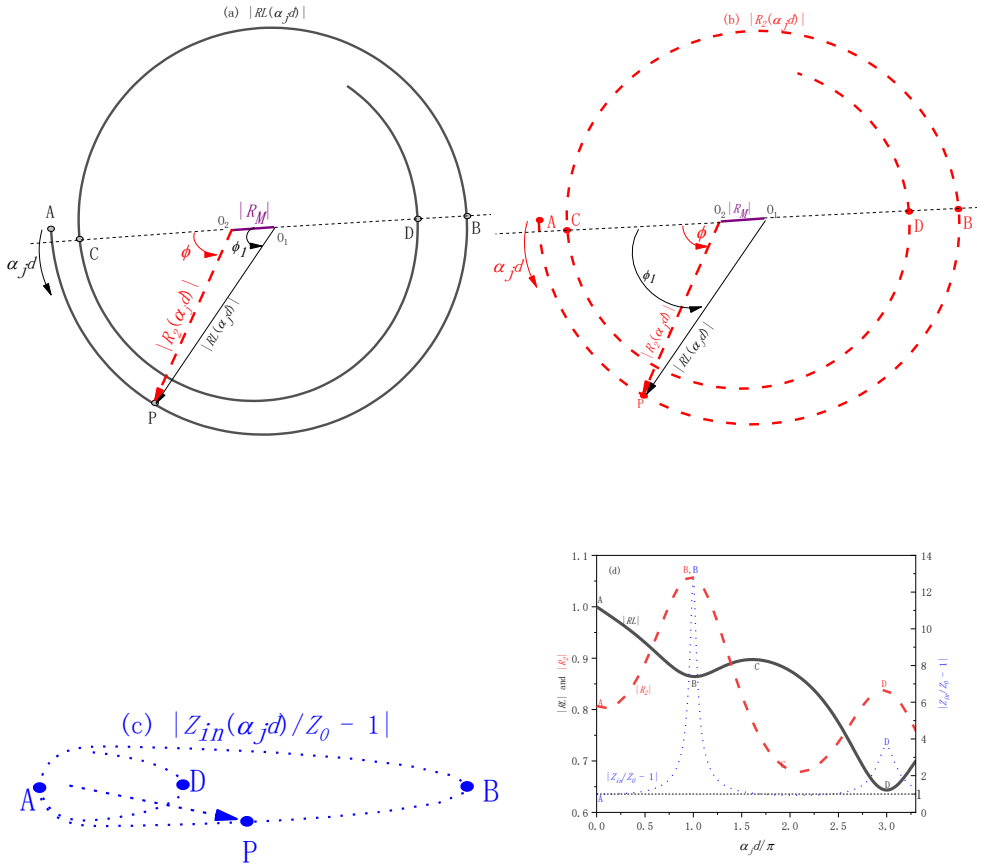

Fig. 5 The curves of $|RL|$, $|R_2|$, and $|Z_{in}/Z_0 - 1|$ referenced to x_1^- at the front interface for MB of Cu@$ZnFe_2O_4$ with fixed $\nu = 4.74$ GHz where $\varepsilon_r = 2.62 - 0.0075j$ and $\mu_r = 1.20 - 0.072j$ [7]. ϕ is the phase difference between beams 1_r and t. Beam 1_r is related to R_M. which equals - 0.193 –

0.014j. The relevant positions are indicated by A, B, C, and D. Point P moves from point A on the curves as d increases from zero. Polar coordinate system has been used for (a – c).

It should be noted that the amplitude of individual beam also contributes an phase effect in wave superposition and such phase contributions have already included in the derivations of the formulae of RL and R_2. $\alpha_j d$ is not the phase of RL and R_2.

In Fig. 5, $RL(x_1^-, \nu, d) = R_M(x_1^-, \nu) + R_2(x_1^-, \nu, d)$ where $R_2 = V(\mathrm{t}, x_1^-)/V(\mathrm{i}, x_1^-)$, $V(\mathrm{k}, x)$ is the voltage of beam k at x. It should be noted that in Fig. 5a, $\mathbf{O_1P} = |RL(\alpha_j d)|\exp(j\alpha_j d) \neq RL(x_1^-, \nu, d)$ since $\alpha_j d$ is not the phase of $R_2(\alpha_j d)$ and $RL(\alpha_j d)$ eventhough $|R_2(x_1^-, \nu, d)| = |\mathbf{O_2P}| = |R_2(\alpha_j d)|$. Thus, $|R_2(\alpha_j d)| = |RL(\alpha_j d) - R_M(\varphi)| = |\mathbf{O_1P} - \mathbf{O_1O_2}|$ where φ is the phase of R_M. In Fig. 5b, $\mathbf{O_2P} = |R_2(\alpha_j d)|\exp(j\alpha_j d) \neq R_2(x_1^-, \nu, d)$ eventhough $|RL(x_1^-, \nu, d)| = |\mathbf{O_1P}| = |RL(\alpha_j d)|$ [54]. Thus, $|RL(\alpha_j d)| = |R_M(\varphi) + R_2(\alpha_j d)| = |\mathbf{O_1O_2} + \mathbf{O_2P}|$. Similarly, the origin of the multi-absorption peaks from the phase effects can be easily seen in Fig. 5. The maxima of $|RL|$ occur when $d = n\lambda_M/2$ (or $\phi = 2n\pi$) where beams 1_r and t are in phase [7]. R_2 is always negative when $d = 0$. $|RL|$ achieves its minima when $d = (2n + 1)\lambda_M/4$ or $\phi = (2n + 1)\pi$ where R_M is negative when $Z_M < Z_0$. Similarly, the minima of $|RL|$ occur when $d = n\lambda_M/2$ or $\phi = (2n + 1)\pi$ where R_M will be positive if $Z_M > Z_0$. The minima of $|RL|$ are thus ensured by the fact that beams 1_r and t are out of phase π [7] rather than by IM or the resonances of material.

The significance of the three conditions mentioned above for the minima of $|RL|$ when $|Z_{in}|$ deviates the most from $|Z_0|$ is demonstrated in Fig. 5 with data from the film of $Cu@ZnFe_2O_4$ [7]. The three curves in Figs. 5a – 5c start from $d = 0$ at point A. When $d = \lambda_M/4$ and $3\lambda_M/4$, point P arrives at points B and D, and beams 1_r and t are out of phase by $\phi = \phi_1 = \pi$ and 3π where $|RL|$ reaches its minima, but $|R_2|$ and $|Z_{in}/Z_0 - 1|$ reach their maxima. When $d = \lambda_M/2$, point P arrives at point C and beams 1_r and t are in phase with $\phi = \phi_1 = 2\pi$. By comparison $|RL|$, $|R_2|$, and $|Z_{in}|$ from Figs. 5a – 5c with those in Fig. 5d, it is seen that full wave cancellations periodically occurred at $\phi = (2n + 1)\pi$ are responsible for the multi-absorptions in film and the absorption mechanism for film is different from that for material. The angular (or phase) effects on beams 1_r, t, and b from film are responsible for the origination of the multi-absorption peaks while the attenuation effect from material [8] only reduces $|R_2|$ monotonically as d increases and ensures that the curve $|R_2(\alpha_j d)|$ in Fig. 5b is a deformed inward spiral. The properties of the material can shift the maximum and minimum positions of $|RL|$ and $|R_2|$ but these shifts can be neglected here for simplicity.

$Z_{in}(x_1^-)$ is large if the voltage $V(x_1^-)$ is large and the current $I(x_1^-)$ is small. As shown by Eqs. 6 - 8, beam t with a large amplitude can ensure a large $Z_{in}(x_1^-)$ when $Z_M < Z_0$. A strong beam t is required since at the minimum position of $|RL(x_1^-)|$, beam t is in phase with beam i and out of phase by π with beams 1_r

when $Z_M < Z_0$, i.e., A strong beam t ensures a large $V(x_1^-)$ from Eq. 6 and a small $I(x_1^-)$ from Eq. 7, thus a large $Z_{in}(x_1^-)$ from Eq. 8.

$$\begin{aligned}\left|V(x_1^-)\right| &= \left|V_{\mathrm{i}}(x_1^-) + V_{\mathrm{l_r}}(x_1^-) + V_{\mathrm{t}}(x_1^-)\right| \\ &= \left|V_{\mathrm{i}}(x_1^-)\right| + [\left|V_{\mathrm{t}}(x_1^-)\right| - \left|V_{\mathrm{l_r}}(x_1^-)\right|]\end{aligned} \tag{6}$$

$$\begin{aligned}\left|I(x_1^-)\right| &= \left|I_{\mathrm{i}}(x_1^-) + I_{\mathrm{l_r}}(x_1^-) + I_{\mathrm{t}}(x_1^-)\right| \\ &= \left|\left|\frac{V_{\mathrm{i}}(x_1^-)}{Z_0}\right| - [\left|\frac{V_{\mathrm{t}}(x_1^-)}{Z_0}\right| - \left|\frac{V_{\mathrm{l_r}}(x_1^-)}{Z_0}\right|]\right|\end{aligned} \tag{7}$$

$$\left|Z_{in}(x_1^-)\right| = \left|\frac{V(x_1^-)}{I(x_1^-)}\right| \tag{8}$$

The reason that IM can usually apply to WMB [7] is that the effect from s_{21} reduces the amplitude of beam t. Three conditions apply to the data shown in Fig. 5 for MB. First, a small value of $\alpha_j d$ ensures that beam t can achieve a large amplitude. Second, $Z_M > Z_0$ is usually achieved at high frequency which makes $\alpha_j d$ large. Thus, the low frequency for $Z_M < Z_0$ can ensure a small value of $\alpha_j d$ at a small value of n in $d = (2n + 1)\lambda_M/4$. Third, if $|R_M| = 0$, $|RL|$ is a monotonic decay function of d when ν is fixed or of ν when d is fixed. Thus, significant absorption peaks are ensured with a significant value of $|R_M|$.

For uniform material, α_P is a constant everywhere within. Thus, the amplitude of the microwaves traveling in material with a distance of x is a monotonic decay function of $\exp(-\alpha_P x)$ which does not initiate an absorption peak. Thus, because of this material effect $|R_2|$ forms an inward spiral curve

in Fig. 5b. However, as shown by Fig. 5d, $|RL|$ can have minimum peaks which signifies that film can absorb more than material. Such absorptions are possible for a small amount of microwave penetration characterized by the amplitude of the penetrating beam and weak attenuation power of material characterized by α_P since the absorption mechanism for film involves the cancellation of beams 1_r and t, and larger cancelation can be achieved by a large number of back-and-forth reflections required by energy conservation. By contrast, the large penetration required by IM results in a weak beam 1_r and a small $|R_M|$ which gives only a shallow $|RL|$ minimum.

$|RL|$ can have minimum peaks as long as wave cancellation is ensured which is achieved when $R_M \neq 0$. As shown by Fig. 5c, $|Z_{in}(x_1^-) - Z_0|$ can still be at its maximum even though $Z_{in}(x_1^-)$ is in phase with Z_0 when point P moves to points B and D. Thus, the minimum values of $|RL(x_1^-)|$ are ensured by the fact that beams t and 1_r are out of phase by π rather than by whether $Z_{in}(x_1^-)$ and Z_0 are in phase.

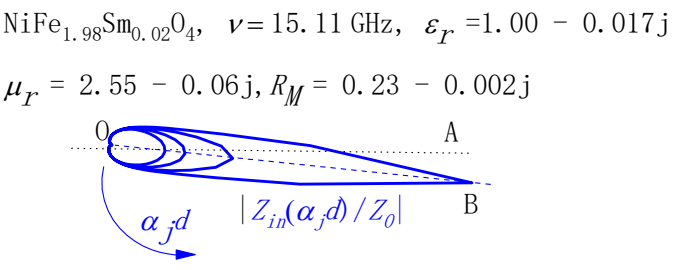

Fig. 6 The curve of $|Z_{in}(\alpha_j d)|$ in the polar coordinate system starts from point O with $d = 0$ and the first maximum of $|Z_{in}(\alpha_j d)|$ is at point B. The information for the curve has been indicated. Line AO shows the direction of vector 1_r. The maxima of $Z_{in}(x_1^-)$ occur on the dotted line OB. At point B, $Z_{in}(x_1^-)$ is significantly larger than Z_0.

In Fig. 6, the maximum positions of $|Z_{in}(\alpha_j d)|$ occur when $\alpha_j d < (2n + 1)\pi$. The maximum positions of $|RL(x_1^-)|$, in this case, should be at $\alpha_j d = (2n + 1)\pi$ where beams t and 1_r are in phase. Similarly, beams t and 1_r being out of phase by π is not always equivalent to $Z_{in}(x_1^-)$ being in phase with Z_0.

In absorption analysis, it is important to note that there is a significant difference between calculations using real and complex numbers. When $Z_M > Z_0 > 0$, then $R_M > 0$ and $|R_M + R_2|$ reaches its maximum value of $|R_M|$ when $|R_2|$ approaches 0 if $R_2 < 0$. However, if R_2 is complex and non-zero, $|R_M + R_2|$ can reach its minimum when $|R_2|$ approaches 0 as ϕ approaches π where $|R_2| \neq 0$. This is a result of the addition of two vectors in opposite directions and one example was provided by Fig. 5a in ref. [7] for the condition of $Z_M > Z_0$.

3. Conclusions

All the problems in the mainstream theory are caused by applying the results of *RL* for film to material. It has been proved from theoretical methods that many concepts such as IM and QWM should be replaced by WCT. In this work, the results obtained previously have been further verified from a different perspective base on the principle presented in section 2.1 with experimental data from a different material, which confirm that film and material must be treated differently. The amplitude of microwaves traveling a distance x in a material can be represented using $\exp(-\alpha_P x)$. The absorption

of film is not determined by the number of cycles of back-and-forth reflections even though it is a feature unique to film but the number of cycles determines the amplitude and phase of beam t. The angular effect from exp(-j$\alpha_j d$) and the amplitude effect of beam t on the value of $|RL(x_1^-)|$ are unique for film and absorption peaks from film are determined by the cancellation of beam 1_r and t. The most efficient absorption occurs when the two beams cancel being out of phase by $(2n + 1)\pi$. Beam t must be the strongest at the minima of $|RL(x_1^-)|$ since it needs to cancel beam 1_r to return the energy to the open space as required by energy conservation. In addition to the absorption effect is contributed by the angular effect of film, which also requires the maximum number of reflections to occur in the film to achieve the maximum amplitude of beam t. The effect of the phase difference between beams 1_r and t on $|RL(x_1^-)|$ is different from that between Z_{in} and Z_0 when $|Z_{in}| \neq |Z_0|$. It can be concluded that the QWM should be replaced by the more accurate inverse relationship found in WCT.

Appendices The expressions for input impedance and the relevant scattering parameters

Appendix A1 Expressions for the metal-backed film

Superscripts – and + indicate positions immediately before and after a position, respectively. Since the voltages and currents are continuous immediately before and after x_1, from Fig. A1 we obtain

$$V(\mathrm{i}, x_1^-) + V(\mathrm{b}, x_1^-) = V(\mathrm{f}_M, x_1^+) + V(\mathrm{b}_M, x_1^+) \tag{A1}$$

$$\frac{1}{Z_0}[V(\mathrm{i}, x_1^-) - V(\mathrm{b}, x_1^-)] = \frac{1}{Z_M}[V(\mathrm{f}_M, x_1^+) - V(\mathrm{b}_M, x_1^+)] \tag{A2}.$$

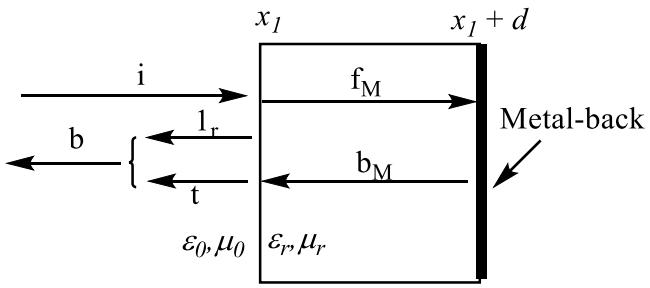

Fig. A1 Metal-backed film with thickness d. i is the incident beam; f_M and b_M are the total forward and backward beams in the film, respectively; 1_r is the reflected beam from the interface at x_1; the transmitted beam t is from beam b_M reflected from the interface at $x_1 + d$; b is the total beam from 1_r and t.

The input impedance Z_{in} for MB is

$$Z_{in}(x_1^-) = Z_0 \frac{V(\mathrm{i}, x_1^-) + V(\mathrm{b}, x_1^-)}{V(\mathrm{i}, x_1^-) - V(\mathrm{b}, x_1^-)} = Z_M \frac{V(\mathrm{f_M}, x_1^+) + V(\mathrm{b_{M,}} x_1^+)}{V(\mathrm{f_M}, x_1^+) - V(\mathrm{b_{M,}} x_1^+)} = Z_{in}(x_1^+)$$

$$= Z_0 \frac{1 + \dfrac{V(\mathrm{b}, x_1^-)}{V(\mathrm{i}, x_1^-)}}{1 - \dfrac{V(\mathrm{b}, x_1^-)}{V(\mathrm{i}, x_1^-)}} = Z_M \frac{1 + \dfrac{V(\mathrm{b_{M,}} x_1^+)}{V(\mathrm{f_M}, x_1^+)}}{1 - \dfrac{V(\mathrm{b_{M,}} x_1^+)}{V(\mathrm{f_M}, x_1^+)}}$$

$$= Z_0 \frac{1 + RL(x_1^-)}{1 - RL(x_1^-)} = Z_M \frac{1 + \dfrac{V(\mathrm{b_{M,}} x_1 + d^-) e^{-j2\pi\nu \frac{\sqrt{\varepsilon_r \mu_r}}{c} d}}{V(\mathrm{f_M}, x_1 + d^-) e^{j2\pi\nu \frac{\sqrt{\varepsilon_r \mu_r}}{c} d}}}{1 - \dfrac{V(\mathrm{b_{M,}} x_1 + d^-) e^{-j2\pi\nu \frac{\sqrt{\varepsilon_r \mu_r}}{c} d}}{V(\mathrm{f_M}, x_1 + d^-) e^{j2\pi\nu \frac{\sqrt{\varepsilon_r \mu_r}}{c} d}}}$$

$$= Z_M \frac{1 + R_M(x_1 + d^-) e^{-j4\pi\nu \frac{\sqrt{\varepsilon_r \mu_r}}{c} d}}{1 - R_M(x_1 + d^-) e^{-j4\pi\nu \frac{\sqrt{\varepsilon_r \mu_r}}{c} d}} = Z_M \frac{1 - e^{-j4\pi\nu \frac{\sqrt{\varepsilon_r \mu_r}}{c} d}}{1 + e^{-j4\pi\nu \frac{\sqrt{\varepsilon_r \mu_r}}{c} d}}$$

$$= Z_M \frac{e^{j2\pi\nu \frac{\sqrt{\varepsilon_r \mu_r}}{c} d} - e^{-j2\pi\nu \frac{\sqrt{\varepsilon_r \mu_r}}{c} d}}{e^{j2\pi\nu \frac{\sqrt{\varepsilon_r \mu_r}}{c} d} + e^{-j2\pi\nu \frac{\sqrt{\varepsilon_r \mu_r}}{c} d}} = -Z_M\, j \tan(2\pi\nu \frac{\sqrt{\varepsilon_r \mu_r}}{c} d) \qquad \text{(A3).}$$

$$= Z_M \tanh(j2\pi\nu \frac{\sqrt{\varepsilon_r \mu_r}}{c} d) = -jZ_M \tan(2\pi\nu \frac{\sqrt{\varepsilon_r \mu_r}}{c} d)$$

From Eq. A3 we obtain

$$Z_0 \frac{1 + RL(x_1^-)}{1 - RL(x_1^-)} = Z_M \frac{1 - e^{-j4\pi\nu \frac{\sqrt{\varepsilon_r \mu_r}}{c} d}}{1 + e^{-j4\pi\nu \frac{\sqrt{\varepsilon_r \mu_r}}{c} d}} \qquad \text{(A4)}$$

Reflection loss $RL(x_1^-)$ can be obtained from Eq. A4.

$$RL(x_1^-) = \frac{V(\mathrm{b}, x_1^-)}{V(\mathrm{i}, x_1^-)} = \frac{Z_{in}(x_1^-) - Z_0}{Z_{in}(x_1^-) + Z_0} = \frac{R_M(x_1^-) - e^{-j4\pi\nu \frac{\sqrt{\varepsilon_r \mu_r}}{c} d}}{1 - R_M(x_1^-) e^{-j4\pi\nu \frac{\sqrt{\varepsilon_r \mu_r}}{c} d}} \qquad \text{(A5)}$$

Appendix A2 Expressions for the film without metal-back

The input impedance Z_{in} for WMB from Fig. A2 is

$$Z_{in}(x_1^-) = Z_0 \frac{V(\mathrm{i}, x_1^-) + V(\mathrm{b}, x_1^-)}{V(\mathrm{i}, x_1^-) - V(\mathrm{b}, x_1^-)} = Z_M \frac{V(\mathrm{f_M}, x_1^+) + V(\mathrm{b_{M,}} x_1^+)}{V(\mathrm{f_M}, x_1^+) - V(\mathrm{b_{M,}} x_1^+)} = Z_{in}(x_1^+)$$

$$= Z_0 \frac{1 + \dfrac{V(\mathrm{b}, x_1^-)}{V(\mathrm{i}, x_1^-)}}{1 - \dfrac{V(\mathrm{b}, x_1^-)}{V(\mathrm{i}, x_1^-)}} = Z_M \frac{1 + \dfrac{V(\mathrm{b_{M,}} x_1^+)}{V(\mathrm{f_M}, x_1^+)}}{1 - \dfrac{V(\mathrm{b_{M,}} x_1^+)}{V(\mathrm{f_M}, x_1^+)}}$$

$$= Z_0 \frac{1 + RL(x_1^-)}{1 - RL(x_1^-)} = Z_M \frac{1 + \dfrac{V(\mathrm{b_{M,}} x_1 + d^-) e^{-j2\pi\nu \frac{\sqrt{\varepsilon_r \mu_r}}{c} d}}{V(\mathrm{f_M}, x_1 + d^-) e^{j2\pi\nu \frac{\sqrt{\varepsilon_r \mu_r}}{c} d}}}{1 - \dfrac{V(\mathrm{b_{M,}} x_1 + d^-) e^{-j2\pi\nu \frac{\sqrt{\varepsilon_r \mu_r}}{c} d}}{V(\mathrm{f_M}, x_1 + d^-) e^{j2\pi\nu \frac{\sqrt{\varepsilon_r \mu_r}}{c} d}}}$$

$$= Z_M \frac{1 + R_M(x_1 + d^-) e^{-j4\pi\nu \frac{\sqrt{\varepsilon_r \mu_r}}{c} d}}{1 - R_M(x_1 + d^-) e^{-j4\pi\nu \frac{\sqrt{\varepsilon_r \mu_r}}{c} d}} = Z_M \frac{1 - R_M(x_1^-) e^{-j4\pi\nu \frac{\sqrt{\varepsilon_r \mu_r}}{c} d}}{1 + R_M(x_1^-) e^{-j4\pi\nu \frac{\sqrt{\varepsilon_r \mu_r}}{c} d}} \quad \text{(A6).}$$

Z_{in} in Eq. A4 for MB is different from that in Eq. A6 for WMB, even though they are related [6]. However, the misuse of transmission-line theory is demonstrated by the fact that Eq. A3 is often wrongly used instead of Eq. A6 for the middle layers in a multi-layered film [55].

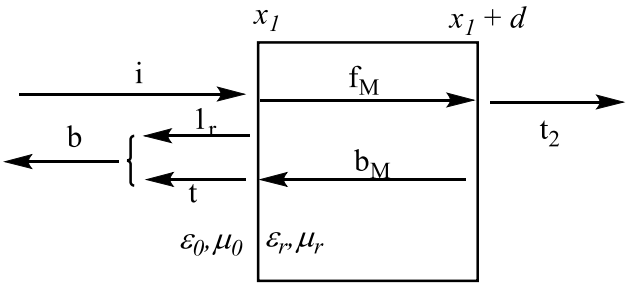

Fig. A2 Film without metal-back. t_2 is the transmitted beam from f_M.

From Eq. A6, we obtain

$$Z_0 \frac{1+s_{11}}{1-s_{11}} = Z_M \frac{1-R_M(x_1^-)e^{-j4\pi\nu\frac{\sqrt{\varepsilon_r\mu_r}}{c}d}}{1+R_M(x_1^-)e^{-j4\pi\nu\frac{\sqrt{\varepsilon_r\mu_r}}{c}d}} \tag{A7}$$

s_{11} can be obtained from Eq. A7.

$$s_{11} = \frac{V(\mathrm{b}, x_1^-)}{V(\mathrm{i}, x_1^-)} = \frac{R_M(x_1^-)(1-e^{-j4\pi\nu\frac{\sqrt{\varepsilon_r\mu_r}}{c}d})}{1-R_M^2(x_1^-)e^{-j4\pi\nu\frac{\sqrt{\varepsilon_r\mu_r}}{c}d}} \tag{A8}$$

From the voltage continuous condition at x_1 of Fig. A2, we obtain

$$V(\mathrm{i}, x_1^-)[1+\frac{V(\mathrm{b}, x_1^-)}{V(\mathrm{i}, x_1^-)}] = V(\mathrm{f_M}, x_1^+)[1+\frac{V(\mathrm{b_M}, x_1^+)}{V(\mathrm{f_M}, x_1^+)}] \tag{A9}$$

Equation A10 can be obtained from Eq. A9.

$$\begin{aligned}(1+s_{11})V(\mathrm{i}, x_1^-) &= [1+\frac{V(\mathrm{b_M}, x_1+d^-)e^{-j2\pi\nu\frac{\sqrt{\varepsilon_r\mu_r}}{c}d}}{V(\mathrm{f_M}, x_1+d^-)e^{j2\pi\nu\frac{\sqrt{\varepsilon_r\mu_r}}{c}d}}][V(\mathrm{f_M}, x_1+d^+)e^{j2\pi\nu\frac{\sqrt{\varepsilon_r\mu_r}}{c}d}] \\ &= [1+R_M(x_1+d^-)e^{-j4\pi\nu\frac{\sqrt{\varepsilon_r\mu_r}}{c}d}]\frac{V_{\mathrm{t_2}}(x_1+d^+)}{\gamma_M(x_1+d^+)}e^{j2\pi\nu\frac{\sqrt{\varepsilon_r\mu_r}}{c}d}\end{aligned} \tag{A10}$$

From Eqs. A8 and A10, we obtain

$$\begin{aligned}s_{21} &= \frac{V(\mathrm{t_2}, x_1+d^+)}{V(\mathrm{i}, x_1^-)} = \frac{(1+s_{11})\gamma_M(x_1+d^+)e^{-j2\pi\nu\frac{\sqrt{\varepsilon_r\mu_r}}{c}d}}{[1-R_M(x_1^-)e^{-j4\pi\nu\frac{\sqrt{\varepsilon_r\mu_r}}{c}d}]} \\ &= \frac{(1+s_{11})[1-R_M(x_1^-)]e^{-j2\pi\nu\frac{\sqrt{\varepsilon_r\mu_r}}{c}d}}{[1-R_M(x_1^-)e^{-j4\pi\nu\frac{\sqrt{\varepsilon_r\mu_r}}{c}d}]} = \frac{[1-R_M^2(x_1^-)]e^{-j2\pi\nu\frac{\sqrt{\varepsilon_r\mu_r}}{c}d}}{1-R_M^2(x_1^-)e^{-j4\pi\nu\frac{\sqrt{\varepsilon_r\mu_r}}{c}d}}\end{aligned} \tag{A11}$$

Acknowledgments

This work was supported by the Foundation of Liaoning Province Education Administration [grant number LJKMZ20221477].

Author contributions

Ying Liu: Conceptualization, Methodology, Validation, Investigation, Resources, Writing - Review & Editing, Supervision, Project administration, Funding acquisition. **Xiangbin Yin**: Data Curation, Investigation. **Michael G. B. Drew**: Conceptualization, Validation, Writing - Review & Editing, Supervision. **Yue Liu**: Conceptualization, Methodology, Validation, Formal analysis, Investigation, Data Curation, Writing - Review & Editing, Visualization.

Conflict of Interest

The authors declare that they have no conflict of interest.

Data availability statement

The data that support the findings of this study are openly available at the following URL/DOI: https://dataverse.harvard.edu/dataverse/BaFe12-iCeiO19-PPy or https://doi.org/10.7910/DVN/NR4IID.

Supplementary information

Available comments and our responses.

References

[1] L. Liang, W. Gu, Y. Wu, B. Zhang, G. Wang, Y. Yang, G. Ji, Heterointerface Engineering in Electromagnetic

Absorbers: New Insights and Opportunities, Adv Mater, 34 (2022) e2106195.

[2] N. Yang, S. Xu, D. Zhang, C. Xu, Super-Wideband Electromagnetic Absorbing TiC/SiOC Ceramic/Glass Composites Derived from Polysiloxane and Titanium Isopropoxide with Low Thickness (<1 mm), Adv. Eng. Mater., (2022) 2201508.

[3] X. Guan, Z. Yang, M. Zhou, L. Yang, R. Peymanfar, B. Aslibeiki, G. Ji, 2D MXene Nanomaterials: Synthesis, Mechanism, and Multifunctional Applications in Microwave Absorption, Small Struct., 3 (2022) 2200102.

[4] P. Liu, Y. Wang, G. Zhang, Y. Huang, R. Zhang, X. Liu, X. Zhang, R. Che, Hierarchical Engineering of Double-Shelled Nanotubes toward Hetero-Interfaces Induced Polarization and Microscale Magnetic Interaction, Adv. Funct. Mater., 32 (2022) 2202588.

[5] P. Liu, G. Zhang, H. Xu, S. Cheng, Y. Huang, B. Ouyang, Y. Qian, R. Zhang, R. Che, Synergistic Dielectric–Magnetic Enhancement via Phase-Evolution

Engineering and Dynamic Magnetic Resonance, Adv. Funct. Mater., 33 (2023) 2211298.
[6] Y. Liu, K. Zhao, M.G.B. Drew, Y. Liu, A theoretical and practical clarification on the calculation of reflection loss for microwave absorbing materials, AIP Adv., 8 (2018) e015223.
[7] Y. Liu, Y. Liu, M.G.B. Drew, A theoretical investigation of the quarter-wavelength model-part 2: verification and extension, Phys. Scr., 97 (2022) 015806.
[8] Y. Liu, Y. Liu, M.G.B. Drew, A Re-evaluation of the mechanism of microwave absorption in film – Part 2: The real mechanism, Mater. Chem. Phys., 291 (2022) 126601.
[9] J. Cheng, H. Zhang, M. Ning, H. Raza, D. Zhang, G. Zheng, Q. Zheng, R. Che, Emerging Materials and Designs for Low- and Multi-Band Electromagnetic Wave Absorbers: The Search for Dielectric and Magnetic Synergy?, Adv. Funct. Mater., 32 (2022) 2200123.

[10] H. Ma, Y. Wang, B. Wang, J. Ding, K. Xu, X. Xia, S. Wei, Synthetic 3D flower-like 1T/2H MoS2@CoFe2O4 composites with enhanced microwave absorption performances, J. Mater. Sci., 58 (2023) 1183-1199.

[11] C.T.A. Xuan, P.T. Tho, T.Q. Dat, N.V. Khien, T.N. Bach, N.T.M. Hong, T.A. Ho, D.T. Khan, H.N. Toan, N. Tran, Development of high-efficiency microwave absorption properties of La1.5Sr0.5NiO4 and SrFe12O19-based materials composites, Surf. Interfaces, 39 (2023) 102890.

[12] Z. Wu, H.W. Cheng, C. Jin, B. Yang, C. Xu, K. Pei, H. Zhang, Z. Yang, R. Che, Dimensional Design and Core-Shell Engineering of Nanomaterials for Electromagnetic Wave Absorption, Adv Mater, 34 (2022) e2107538.

[13] M. Cao, C. Han, X. Wang, M. Zhang, Y. Zhang, J. Shu, H. Yang, X. Fang, J. Yuan, Graphene nanohybrids: excellent electromagnetic properties for the absorbing and shielding of electromagnetic waves, J. Mater. Chem. C, 6 (2018) 4586-4602.

[14] Y. Liu, Y. Liu, M.G.B. Drew, A Re-evaluation of the mechanism of microwave absorption in film – Part 1: Energy conservation, Mater. Chem. Phys., 290 (2022) 126576.

[15] Y. Liu, Y. Liu, M.G.B. Drew, A re-evaluation of the mechanism of microwave absorption in film – Part 3: Inverse relationship, Mater. Chem. Phys., 290 (2022) 126521.

[16] Y. Liu, Y. Lin, K. Zhao, M.G.B. Drew, Y. Liu, Microwave absorption properties of Ag/NiFe2-xCexO4 characterized by an alternative procedure rather than the main stream method using “reflection loss”, Mater. Chem. Phys., 243 (2020) e122615.

[17] X. Wang, Z. Du, M. Hou, Z. Ding, C. Jiang, X. Huang, J. Yue, Approximate solution of impedance matching for nonmagnetic homogeneous absorbing materials, The European Physical Journal Special Topics, 231 (2022) 4213-4220.

[18] S. Zhang, T. Wang, M. Gao, P. Wang, H. Pang, L. Qiao, F. Li, Strict proof and applicable range of the

quarter-wavelength model for microwave absorbers, J. Phys. D: Appl. Phys., 53 (2020) 265004.
[19] S. Zhu, K. Huang, J. Ni, X. Kan, Q. Lv, Y. Cheng, S. Feng, X. Liu, Magnetic and microwave absorption properties of Ni0.6Zn0.4Fe2O4 /SrFe12O19 composites, Mater. Chem. Phys., 288 (2022) 126398.
[20] Y. Wang, X. Li, X. Han, P. Xu, L. Cui, H. Zhao, D. Liu, F. Wang, Y. Du, Ternary Mo2C/Co/C composites with enhanced electromagnetic waves absorption, Chem. Eng. J., 387 (2020) 124159.
[21] Z. Cai, Y. Ma, K. Zhao, M. Yun, X. Wang, Z. Tong, M. Wang, J. Suhr, L. Xiao, S. Jia, X. Chen, Ti3C2Tx MXene/graphene oxide/Co3O4 nanorods aerogels with tunable and broadband electromagnetic wave absorption, Chem. Eng. J., 462 (2023) 142042.
[22] G. Yang, B. Wen, Y. Wang, X. Zhou, X. Liu, S. Ding, In situ construction of ZIF-67 derived Mo2C@cobalt/carbon composites toward excellent electromagnetic wave absorption properties, Nanotechnology, 34 (2023) 185704.

[23] Y. Sun, N. Wang, H. Yu, X. Jiang, Metal–organic framework-based Fe/C@Co3O4 core–shell nanocomposites with outstanding microwave absorption properties in low frequencies, J. Mater. Sci., 55 (2020) 7304-7320.

[24] Y. Sun, H. Jia, J. Liu, H. Yu, X. Jiang, Metal–organic framework-derived C/Co/Co3O4 nanocomposites with excellent microwave absorption properties in low frequencies, J. Mater. Sci.: Mater. Electron., 31 (2020) 11700-11713.

[25] Y. Liu, Y. Liu, M.G.B. Drew, A theoretical investigation on the quarter-wavelength model — Part 1：Analysis, Phys. Scr., 96 (2021) 125003.

[26] M. Green, X. Chen, Recent progress of nanomaterials for microwave absorption, J. Materiomics, 5 (2019) 503-541.

[27] Y. Liu, M.G.B. Drew, H. Li, Y. Liu, A theoretical analysis of the relationships shown from the general experimental results of scattering parameters s11 and

s21 -- Exemplified by the film of BaFe12-iCeiO19/polypyrene with i = 0.2, 0.4, 0.6, J. Microwave Power Electromagn. Energy, 55 (2021) 197–218.

[28] K.A. Aly, Comment on the relationship between electrical and optical conductivity used in several recent papers published in the journal of materials science: materials in electronics, J. Mater. Sci.: Mater. Electron., 33 (2022) 2889-2898.

[29] Y. Liu, Y. Liu, M.G.B. Drew, Natural Mathematical Derivation of the Gibbs–Duhem Equation Related to ΔG and ∂G/∂ξ, Int. J. Thermophys., 43 (2022) 73.

[30] Y. Liu, M.G.B. Drew, H. Li, Y. Liu, An experimental and theoretical investigation into methods concerned with “reflection loss” for microwave absorbing materials, Mater. Chem. Phys., 243 (2020) 122624.

[31] Y. Liu, M.G.B. Drew, Y. Liu, BaFe11.8Ce0.2O19/PPy, Harvard Dataverse, 2021, doi/10.7910/DVN/NR4IID.

[32] Numerical calculations were carried out using internal software which is available. Please contact Prof. Yue Liu (Email: yueliusd@163.com) for further details.
[33] Y. Liu, M.G.B. Drew, Y. Liu, Characterization microwave absorption from active carbon/BaSmxFe12−xO19/polypyrrole composites analyzed with a more rigorous method, J. Mater. Sci.: Mater. Electron., 30 (2019) 1936-1956.
[34] T. Wang, R. Han, G. Tan, J. Wei, L. Qiao, F. Li, Reflection loss mechanism of single layer absorber for flake-shaped carbonyl-iron particle composite, J. Appl. Phys., 112 (2012) e104903.
[35] T. Wang, H. Wang, G. Tan, L. Wang, L. Qiao, The Relationship of Permeability and Permittivity at the Perfect Matching Point of Electromagnetic Wave Absorption for the Absorber Filled by Metallic Magnetic Particles, IEEE Trans. Magn., 51 (2015) e2800405.
[36] B. Li, F. Wang, K. Wang, J. Qiao, D. Xu, Y. Yang, X. Zhang, L. Lyu, W. Liu, J. Liu, Metal sulfides based composites as promising efficient microwave absorption

materials: A review, Journal of Materials Science & Technology, 104 (2022) 244-268.
[37] P. Wang, D. Liu, L. Cui, B. Hu, X. Han, Y. Du, A review of recent advancements in Ni-related materials used for microwave absorption, J. Phys. D: Appl. Phys., 54 (2021) 473003.
[38] H. Wei, Y. Tian, Q. Chen, D. Estevez, P. Xu, H.-X. Peng, F. Qin, Microwave absorption performance of 2D Iron-Quinoid MOF, Chem. Eng. J., 405 (2021) 126637.
[39] Y. Zhao, X. Zuo, Y. Guo, H. Huang, H. Zhang, T. Wang, N. Wen, H. Chen, T. Cong, J. Muhammad, X. Yang, X. Wang, Z. Fan, L. Pan, Structural Engineering of Hierarchical Aerogels Comprised of Multi-dimensional Gradient Carbon Nanoarchitectures for Highly Efficient Microwave Absorption, Nano-micro Lett, 13 (2021) 144.
[40] Z. Zhang, Z. Cai, Z. Wang, Y. Peng, L. Xia, S. Ma, Z. Yin, Y. Huang, A Review on Metal-Organic Framework-Derived Porous Carbon-Based Novel Microwave Absorption Materials, Nano-micro Lett, 13 (2021) 56.

[41] X. Zhang, J. Qiao, Y. Jiang, F. Wang, X. Tian, Z. Wang, L. Wu, W. Liu, J. Liu, Carbon-Based MOF Derivatives: Emerging Efficient Electromagnetic Wave Absorption Agents, Nano-micro Lett, 13 (2021) 135.

[42] M. Liu, R. Tian, H. Chen, S. Li, F. Huang, K. Peng, H. Zhang, One-dimensional chain-like MnO@Co/C composites for high-efficient electromagnetic wave absorbent, J. Magn. Magn. Mater., 499 (2020) e166289.

[43] J. Qiao, D. Xu, L. Lv, X. Zhang, F. Wang, W. Liu, J. Liu, Self-Assembled ZnO/Co Hybrid Nanotubes Prepared by Electrospinning for Lightweight and High-Performance Electromagnetic Wave Absorption, ACS Appl. Nano Mater., 1 (2018) 5297-5306.

[44] B. Zhao, Y. Li, X. Guo, R. Zhang, J. Zhang, H. Hou, T. Ding, J. Fan, Z. Guo, Enhanced electromagnetic wave absorbing nickel (Oxide)-Carbon nanocomposites, Ceram. Int., 45 (2019) 24474-24486.

[45] M. Hu, H. Xing, R. Shi, X. Ji, Electromagnetic wave absorption of hierarchical porous MWCNTs@ZnO/NiO composites enhanced by multiple polarization and

dielectric loss, J. Mater. Sci.: Mater. Electron., 31 (2020) 17339-17350.

[46] N. Gao, W.P. Li, W.S. Wang, D.P. Liu, Y.M. Cui, L. Guo, G.S. Wang, Balancing Dielectric Loss and Magnetic Loss in Fe-NiS2/NiS/PVDF Composites toward Strong Microwave Reflection Loss, ACS Appl Mater Interfaces, 12 (2020) 14416-14424.

[47] L.L. Liang, G. Song, Z. Liu, J.P. Chen, L.J. Xie, H. Jia, Q.Q. Kong, G.H. Sun, C.M. Chen, Constructing Ni12P5/Ni2P Heterostructures to Boost Interfacial Polarization for Enhanced Microwave Absorption Performance, ACS Appl Mater Interfaces, 12 (2020) 52208-52220.

[48] Y. Huang, J. Ji, Y. Chen, X. Li, J. He, X. Cheng, S. He, Y. Liu, J. Liu, Broadband microwave absorption of Fe3O4BaTiO3 composites enhanced by interfacial polarization and impedance matching, "Composites, Part B", 163 (2019) 598-605.

[49] H. Xie, C. Yang, Y. Zhou, Z. Ren, P. Liu, High-efficiency and ultra-thin electromagnetic wave absorption

xAl2O3–(1 − x)Sr0.85Gd0.15TiO3 ceramics in X-band, J. Mater. Sci.: Mater. Electron., 31 (2020) 16178-16188.
[50] H. Xing, Y. Wang, L. Bai, X. Ji, P. Yang, Fabrication of ZnS/C microsphere composites with enhanced electromagnetic wave absorption properties, J. Mater. Sci.: Mater. Electron., 33 (2022) 20021-20034.
[51] H. Wei, X. Yin, X. Li, M. Li, X. Dang, L. Zhang, L. Cheng, Controllable synthesis of defective carbon nanotubes/Sc2Si2O7 ceramic with adjustable dielectric properties for broadband high-performance microwave absorption, Carbon, 147 (2019) 276-283.
[52] F. Wang, Y. Liu, H. Zhao, L. Cui, L. Gai, X. Han, Y. Du, Controllable seeding of nitrogen-doped carbon nanotubes on three-dimensional Co/C foam for enhanced dielectric loss and microwave absorption characteristics, Chem. Eng. J., 450 (2022) 138160.
[53] Y. Liu, C. Tian, F. Wang, B. Hu, P. Xu, X. Han, Y. Du, Dual-pathway optimization on microwave absorption characteristics of core–shell Fe3O4@C microcapsules: Composition regulation on magnetic core and MoS2

nanosheets growth on carbon shell, Chem. Eng. J., 461 (2023).

[54] Y. Liu, Y. Ding, Q. Chen, Y. Liu, Preparation of NiFe2-xMxO4(M=Ce,Sm,Gd) and microwave absorption properties of its films, Journal of Shenyang Normal University (Natural Science Edition), 41 (2023) 98 - 103.

[55] M.F. Elmahaishi, R.a.S. Azis, I. Ismail, F.D. Muhammad, A review on electromagnetic microwave absorption properties: their materials and performance, J. Mater. Res. Technol., 20 (2022) 2188-2220.

Supplementary Files

This is a list of supplementary files associated with this preprint. Click to download.

- SupplementaryMaterialsJMSCD2301012.pdf